Published in final edited form as:
Dev Biol. 2010 November 1; 347(1): 133–146. doi:10.1016/j.ydbio.2010.08.015.

Twist1 activity thresholds define multiple functions in limb development

Dayana Krawchuk[1,@], **Shoshana J. Weiner**[1], **You-Tzung Chen**[2,#], **Benson Lu**[1], **Frank Costantini**[1], **Richard R. Behringer**[2], and **Ed Laufer**[1,3,*,%]

[1]Department of Genetics and Development, Columbia University Medical Center, New York, NY 10032, USA

[2]Department of Genetics, The University of Texas MD Anderson Cancer Center, Houston, TX 77030, USA

[3]Department of Pathology and Cell Biology, Columbia University Medical Center, New York, NY 10032, USA

Summary

The basic helix-loop-helix transcription factor Twist1 is essential for normal limb development. *Twist1*$^{-/-}$ embryos die at midgestation. However, studies on early limb buds found that *Twist1*$^{-/-}$ mutant limb mesenchyme has an impaired response to FGF signaling from the apical ectodermal ridge, which disrupts the feedback loop between the mesenchyme and AER, and reduces and shifts anteriorly *Shh* expression in the zone of polarizing activity. We have combined *Twist1* null, hypomorph and conditional alleles to generate a *Twist1* allelic series that survives to birth. As Twist1 activity is reduced, limb skeletal defects progress from preaxial polydactyly to girdle reduction combined with hypoplasia, aplasia or mirror symmetry of all limb segments. With reduced Twist1 activity there is striking and progressive upregulation of ectopic *Shh* expression in the anterior of the limb, combined with an anterior shift in the posterior *Shh* domain, which is expressed at normal intensity, and loss of the posterior AER. Consequently limb outgrowth is initially impaired, before an ectopic anterior Shh domain expands the AER, promoting additional growth and repatterning. Reducing the dosage of FGF targets of the Etv gene family, which are known repressors of *Shh* expression in the anterior limb mesenchyme, strongly enhances the anterior skeletal phenotype. Conversely this and other phenotypes are suppressed by reducing the dosage of the Twist1 antagonist *Hand2*. Our data support a model whereby multiple Twist1 activity thresholds contribute to early limb bud patterning, and suggest how particular combinations of skeletal defects result from differing amounts of Twist1 activity.

Keywords

limb; Twist1; pattern; signaling center; ZPA; AER

*Author for correspondence (elaufer@columbia.edu).
Present address: @Department of Human Genetics, McGill University, Montreal, Quebec H3G 1Y6, Canada
#Graduate Institute of Clinical Genomics, National Taiwan University College of Medicine, Taipei 10055, Taiwan
%Department of Pathology and Cell Biology, Columbia University Medical Center, New York, NY 10032, USA

Introduction

Limb patterning is coordinated by discrete signaling centers, located within the limb mesenchyme or overlying ectoderm (reviewed in (Zeller et al., 2009)). Anteroposterior patterning is primarily regulated by Sonic hedgehog (Shh) produced within the posterior mesenchymal zone of polarizing activity (ZPA) (Riddle et al., 1993), while proximodistal outgrowth is regulated by fibroblast growth factor (FGF) signals produced by the distal ectodermal apical ectodermal ridge (AER) (Fallon et al., 1994; Niswander et al., 1993). Patterning requires both appropriate responses to these signals, and precise temporally and spatially regulated signal expression. Thus ectopic Shh expression in anterior limb mesenchyme causes preaxial polydactyly (Riddle et al., 1993), while AER disruptions lead to skeletal element loss (Boulet et al., 2004; Saunders, 1948; Sun et al., 2002).

Shh expression is regulated by combinatorial interactions between positive and negative transcription factors and growth factor signaling. Posterior mesenchyme is made competent to express *Shh* by multiple transcription factors (Davenport et al., 2003; te Welscher et al., 2002; Zakany et al., 2004). These work in concert with AER-derived FGF signals to induce *Shh* expression, although whether secondary signals downstream of FGF are required for *Shh* expression has not been determined. Shh expression is maintained in competent tissue by a positive feedback loop between Shh and Fgf4/Fgf8 in the posterior AER (Laufer et al., 1994; Niswander et al., 1994). Competence factors for Shh expression include Hand2 and Tbx3, which are expressed in posterior limb mesenchyme, initially in response to primary axial patterning cues, and later in response to Shh signaling (Charite et al., 2000; Davenport et al., 2003; Fernandez-Teran et al., 2000; te Welscher et al., 2002). *Shh* expression is prevented in anterior and distal limb mesenchyme by other transcription factors, including Alx4 (Qu et al., 1997), and the Ets family proteins Etv4 (Pea3) and Etv5 (Erm) that act downstream of AER-derived FGF signals (Mao et al., 2009; Zhang et al., 2009). Thus *Shh* expression reflects a balance between positively and negatively acting factors that position the *Shh* expression domain along the anteroposterior and proximodistal axes.

Twist1 is a bHLH transcription factor implicated as a regulator of limb development (Cai and Jabs, 2005; Chen and Behringer, 1995; O'Rourke et al., 2002; Zuniga et al., 2002). *Twist1* is expressed in lateral plate mesenchyme prior to limb outgrowth and becomes progressively restricted to the peripheral mesenchyme within the limb. In *Twist1*$^{-/-}$ mice forelimb growth is stunted (Chen and Behringer, 1995), which correlates with failure of AER maintenance, and induction of ectopic posterior mesenchymal cell death (O'Rourke et al., 2002; Zuniga et al., 2002). Molecular marker analysis suggests a positive feedback loop between Fgf10 in the mesenchyme and Fgf8 in the AER breaks down, as *Fgfr1* expression is lost from *Twist1*$^{-/-}$ limb mesenchyme. *Shh* expression is severely reduced and shifted to more distal mesenchyme in *Twist1*$^{-/-}$ forelimbs. Expression of several Shh- and FGF-dependent patterning genes is also abnormal (O'Rourke et al., 2002; Zuniga et al., 2002). A number of genes apparently downstream of *Twist1*, including Alx family genes, have been identified (Loebel et al., 2002). However the functional significance and specificity of these gene expression changes has not been assessed because *Twist1*$^{-/-}$ embryos die by embryonic day (E) 10.5, prior to significant limb outgrowth.

Genetic evidence suggests that Twist1 also negatively regulates Shh signaling and/or *Shh* expression in anterior limb mesenchyme. *Twist1*$^{+/-}$ mice or human Saethre-Chotzen syndrome (SCS) patients who display a TWIST1 haploinsufficiency have mild, and variable, distal limb abnormalities (Bourgeois et al., 1998; Cai and Jabs, 2005; Firulli et al., 2005). These include hindlimb preaxial polydactyly, which is bilateral in 25% of *Twist1*$^{+/-}$ mice (Bourgeois et al., 1998). The murine polydactyly is completely suppressed by reducing the gene dosage of *Hand2*, a member of the *Twist* bHLH family that is a positive regulator of Shh expression

(Firulli et al., 2005). In chick limbs *Twist1* overexpression can reduce the severity of *Hand2*-induced preaxial polydactyly (Firulli et al., 2005). While an antagonistic balance between Twist1 and Hand2 activities is thus required for normal anteroposterior patterning, the molecular changes are not well described because of the low expressivity of the $Twist1^{+/-}$ phenotype.

Comparing the $Twist1^{+/-}$ morphological phenotype with the $Twist1^{-/-}$ molecular phenotype raises inconsistencies that suggest relatively complex functions for *Twist1* in early limb development. Notably, more severe phenotypes than mild hindlimb polydactyly would be predicted from the changes in both forelimb and hindlimb gene expression patterns observed in null mutant embryos. Recently a novel murine *Twist1* allele was identified in an ENU mutagenesis screen. Charlie Chaplin ($Twist1^{CC}$) encodes an S192P amino acid substitution that disrupts the function of a C-terminal protein interaction domain (Bialek et al., 2004). Fifty-two percent of $Twist1^{CC/+}$ mice were reported to have bilateral hindlimb polydactyly, while $Twist1^{CC/CC}$ mice have short limbs and hindlimb polydactyly, but die perinatally. Thus $Twist1^{CC}$ mutants are affected relatively severely and survive long enough to allow the integrated analysis of *Twist1* morphological and molecular phenotypes.

We generated a *Twist1* allelic series using $Twist1^{CC}$ and $Twist1^{-}$ mutant alleles to ask how progressively reducing Twist1 activity affects limb development and patterning. *Twist1* mutant phenotypes include discrete temporal and spatial molecular defects, with concordant and dramatic changes in limb and girdle cartilage pattern. Furthermore we find that Twist1 positions the posterior *Shh* domain along the anteroposterior axis in a dosage sensitive manner and is a major negative regulator of *Shh* expression in the anterior limb. Twist1 apparently exerts its effects through a network of transcription factors that include Etv and Alx family genes, each of which contributes to aspects of the *Twist1* phenotype. We provide a model that shows how posterior defects in early signaling center regulation can cause loss of anterior skeletal elements, and that is consistent with different thresholds of Twist1 activity regulating different aspects of limb patterning.

Materials and Methods

Mouse strains and genotyping

Animal experiments were performed according to Columbia University Institutional Animal Care guidelines. Noon on the day of the mating plug was considered E0.5. $Hand2^{-}$ (Srivastava et al., 1997), $Twist1^{tm1Bhr}$ ($Twist1^{-}$; (Chen and Behringer, 1995), Shh^{LacZ} (Shh^{-}; (Jeong et al., 2004), $Twist1^{Skam10Jus}$ ($Twist1^{CC}$; (Bialek et al., 2004), $Twist1^{flox}$ (Chen et al., 2007), $Prx1\text{-}cre^{Tg}$ (Logan et al., 2002), $Etv4^{tm1Arbr}$ ($Etv4^{-}$; (Livet et al., 2002) and $Etv5^{LacZ}$ ($Etv5^{-}$; (Lu et al., 2009) alleles were maintained on B6, 129Sv or 129Sv.B6 backgrounds. Mice were genotyped by PCR, and $Twist1^{CC}$ T707C substitutions were confirmed by sequencing.

Skeletal stains, digit scoring and in situ hybridization

Bone/cartilage stains were performed using Alcian blue/alizarin red S staining as described (Webb and Byrd, 1994). Digits were scored on the basis of phalange number and morphology (Patton and Kaufman, 1995). Whole-mount and section in situ hybridization was performed as described (Laufer et al., 1997). All gene expression analyses were performed on 3 or more limbs. Riboprobes used: *Fgf8* (Crossley and Martin, 1995), *Shh* (Roelink et al., 1994), *Twist1* (Chen and Behringer, 1995), *Hand2* (Srivastava et al., 1995), *HoxA11* (Davis et al., 1995), *HoxD11* (Burke et al., 1995), *Ptch1* (Marigo et al., 1996), *Tbx2* (Chapman et al., 1996), *Tbx3* (Chapman et al., 1996), *Spry1* (Zhang et al., 2001), *Pax1* (Balling et al., 1988), *Fgfr1* (Peters et al., 1992), *Etv5* (Chotteau-Lelievre et al., 2001), *Alx4* (te Welscher et al., 2002), *Gli1* (Hui et al., 1994), c*Spry1* (Minowada et al., 1999), c*Shh* (Riddle et al., 1993).

Chick limb experiments

Fertile SPF White Leghorn chicken eggs (Charles River) were incubated at 37.5°C in a humidified incubator and staged according to Hamburger and Hamilton (Hamburger and Hamilton, 1951). Stage 20 forelimb buds were infected with replication-defective activated Fgfr1 virus (Fgfr1*, RIS-pm174HA; (Liu et al., 2001), and limbs harvested up to 42 h later. In some experiments the posterior AER was removed (Laufer et al., 1994) prior to retroviral infection. The AMV-3C2 viral gag antibody was obtained from the Developmental Studies Hybridoma Bank. Section immunohistochemistry was performed as described (Vargesson et al., 2001).

Results

Effects of altering Twist1 activity on limb cartilage patterns

We performed the appropriate genetic crosses to generate *Twist1*$^{CC/+}$, *Twist1*$^{+/-}$, *Twist1*$^{CC/CC}$ and *Twist1*$^{CC/-}$ mutant animals. We previously found that 25% of hindlimbs in our *Twist1*$^{+/-}$ animals were polydactylous with one ectopic preaxial digit (Firulli et al., 2005). By contrast 82% of *Twist1*$^{CC/+}$ hindlimbs had one or two ectopic preaxial digits (Figs. 1M, Fig. 2Ac), whether on a 129, B6, or 129.B6 background. Thus while *Twist1*$^{CC/+}$ and *Twist1*$^{+/-}$ heterozygote phenotypes are similar, the *Twist1*$^{CC/+}$ phenotype is more penetrant.

Both *Twist1*$^{CC/CC}$ and *Twist1*$^{CC/-}$ mice died immediately after birth. They displayed gross limb, ventral body wall, skull and neural tube closure defects that were more severe in the *Twist1*$^{CC/-}$ animals (Figs. S1, Fig. S2). Skeletal preparations at E17.5 and E18.5 revealed multiple forelimb and hindlimb abnormalities, as well as defects in the scapula, clavicle and pelvic girdle (Fig. 1, Table 1). *Twist1*$^{CC/CC}$ forelimbs frequently had four digits with apparent posteriorized preaxial duplications (Fig. 1P). Their radii were hypoplastic or aplastic (Fig. 1O), and their humeruses lacked deltoid tuberosities (Fig. 1O). *Twist1*$^{CC/-}$ forelimbs had as few as 3 digits, with striking mirror symmetry along the anteroposterior axis (Fig. 1DD). They also had radial hypoplasia or aplasia, or an apparently duplicated ulna (Fig. 1CC). *Twist1*$^{CC/-}$ humeruses were severely hypoplastic (Fig. 1CC).

The difference between *Twist1*$^{CC/CC}$ and *Twist1*$^{CC/-}$ hindlimbs was less pronounced than for forelimbs. Hindlimbs had five or fewer digits, with digit I always replaced by a more posterior digit; other digit identities were hard to define (Fig. 1T,HH; Table 1). The tibia was always absent in *Twist1*$^{CC/CC}$ or *Twist1*$^{CC/-}$ animals, but the femurs appeared normal (Fig. 1S,GG).

Twist1$^{CC/CC}$ and *Twist1*$^{CC/-}$ shoulder and pelvic girdles were also abnormal, with *Twist1*$^{CC/-}$ skeletons again more severely affected. Scapular phenotypes ranged from moderate hypoplasia with reduced acromion processes (Fig. 1Q), to almost complete aplasia (Fig. 1EE). Clavicles were also reduced, primarily within the medial endochondral segment (Fig. 1R,FF). Within the pelvic girdle the phenotypes ranged from hypoplasia to loss of the pubic bone exclusively (Fig. 1U,II). Taken together these data reveal a complex set of limb and girdle phenotypes that affect elements at all proximodistal levels and that also impact anteroposterior identities. The progressive severity of the phenotypes across this *Twist1* allelic series is also consistent with a correlated progressive reduction in Twist1 function.

Despite the severity of the *Twist1*$^{CC/-}$ phenotype, these results do not reflect complete loss of Twist1 activity in the limb bud. We therefore used a floxed conditional null allele of Twist1 (*Twist1*^{Fx}) in combination with the *Prx1-cre* transgene driver (Logan et al., 2002), to attempt complete removal of Twist1 activity from the limb mesenchyme. We generated both *Prx1-cre;Twist1*$^{CC/Fx}$ and *Prx1-cre;Twist1*$^{Fx/-}$ embryos. *Prx1-cre;Twist1*$^{CC/Fx}$ limbs resemble *Twist1*$^{CC/CC}$ limbs (Fig. 1V–BB, Table 1), whereas *Prx1-cre;Twist1*$^{Fx/-}$ limbs resemble *Twist1*$^{CC/-}$ limbs (Fig. 1JJ-PP, S3; Table 1). Notably *Prx1-cre;Twist1*$^{Fx/-}$ limbs can have a

duplicated ulna and handplate, and severely reduced scapula and clavicle (Fig. 1JJ,LL,MM). Interestingly, pelvic defects are restricted to the ischium, rather than the pubis as in *Twist1*$^{CC/CC}$ and *Twist1*$^{CC/-}$ mutants (Fig. 1PP). If deletion of the conditional *Twist1* allele is complete, then *Prx1-cre;Twist1*$^{CC/Fx}$ should phenocopy *Twist1*$^{CC/-}$ in the limb. That it more closely resembles *Twist1*$^{CC/CC}$, suggests that some residual Twist1 activity is present. Nonetheless these data provide evidence that the *Twist1*^{CC} allele is not significantly neomorphic, as the *Prx1-cre;Twist1*$^{Fx/-}$ phenotype recapitulates the range of limb and girdle defects associated with the *Twist1*^{CC} allele.

Twist1^{CC} phenotypes are sensitive to *Hand2* gene dosage

If *Twist1*^{CC} is functioning in normal *Twist1* pathways, it should display genetic interactions similar to *Twist1*. We therefore asked if reducing *Hand2* dosage in the context of *Twist1*^{CC} allelic combinations reduced their severity, as Hand2 null heterozygosity completely suppresses *Twist1*$^{+/-}$ hindlimb polydactyly (Firulli et al., 2005).

We crossed a *Hand2* null allele onto *Twist1*^{CC} mutant backgrounds and scored the resultant skeletal phenotypes (Fig. 2, Table 1). Several aspects of the *Twist1*^{CC} phenotype were sensitive to *Hand2* dosage. *Twist1*$^{CC/+}$ hindlimb polydactyly (n=131/160; 82% of hindlimbs) is completely suppressed by lowering Hand2 dosage (*Twist1*$^{CC/+}$;Hand2$^{+/-}$: 0/130; 0%; Fig. 2A). The *Twist1*$^{CC/-}$;*Hand2*$^{+/-}$ forelimbs resembled those of the *Twist1*$^{CC/CC}$ genotype, as often digit number increased, the radius was absent, the ulna was not duplicated, and the humerus was more complete (Fig. 2B, Table 1). The *Twist1*$^{CC/-}$;*Hand2*$^{+/-}$ pubis was more complete than in *Twist1*$^{CC/-}$; *Hand2*$^{+/+}$ animals (Fig. 2B,C; Table 1), and clavicle length was increased (data not shown). However *Hand2* null heterozygosity never completely rescued a *Twist1*$^{CC/CC}$ or *Twist1*$^{CC/-}$ phenotype. Taken together these data provide additional evidence that the *Twist1*^{CC} allele acts in similar pathways to wild type *Twist1*. They furthermore indicate that balanced antagonism between Twist1 and Hand2 is critical for regulating development along the entire limb proximodistal axis.

Twist1 and Hand2 activities converge to regulate Shh signaling

Preaxial polydactyly is a hallmark of ectopic Shh signaling. Thus reducing Twist1 activity might lead to either ectopic *Shh* expression or activation of Shh signaling. We therefore examined the expression of *Shh* and the Shh targets in *Twist1*$^{CC/+}$ and *Twist1*$^{CC/+}$;*Hand2*$^{+/-}$ hindlimbs at E11-E12, when *Twist1*$^{CC/+}$ ectopic anterior outgrowths are first observed (Fig. 3). In *Twist1*$^{CC/+}$ hindlimbs we detected ectopic anterior *Shh* expression at the base of the autopod at low frequency (n=2/23 limbs, Fig. 3A,B), similar to a previous report that a small subset of *Twist1*$^{+/-}$ hindlimbs had ectopic *Shh* expression (O'Rourke et al., 2002). By contrast the Shh targets *Gli1* and *Hand2* in limb mesenchyme and the indirect target *Fgf4* in the overlying AER were each induced in 50%–75% of limbs (n=74/106 limbs in total, Fig. 3A,B). This suggests that ectopic *Shh* expression is induced in most *Twist1*$^{CC/+}$ hindlimbs, but at a level that we cannot detect. We never observed ectopic gene expression in *Twist1*$^{CC/+}$;*Hand2*$^{+/-}$ limbs (n=0/27 limbs; Fig. 3B), consistent with their normal skeletal morphology at later ages. The similar frequencies of ectopic Shh target expression and hindlimb polydactyly (82%, Fig. 2A) support the idea that Twist1 and Hand2 activities converge at the level of Shh signaling, and possibly upstream of ectopic Shh expression.

To test this directly, we intercrossed *Twist1*$^{CC/+}$ and *Shh*$^{+/-}$ animals, and scored the frequency of hindlimb polydactyly in their offspring (Fig. 3C). 21 of 32 *Twist1*$^{CC/+}$ hindlimbs had preaxial polydactyly, while a significantly reduced 4 of 22 *Twist1*$^{CC/+}$;*Shh*$^{+/-}$ hindlimbs ($p<0.0001$) were polydactylous. Reducing *Shh* dosage also reduced the severity of the polydactyly: none of the double mutant limbs had an ectopic digit 2, compared to two-thirds of the *Twist1* single

mutants. These results provide evidence that high levels of *Twist1* activity are required primarily to repress *Shh* expression in anterior limb mesenchyme.

Signaling center defects in *Twist1*^{CC} compound mutant limb buds

To better understand the changes underlying the more complex skeletal phenotypes of the compound *Twist1* mutants, we analyzed limb buds during the time when pattern is established. From E9.5 *Twist1*$^{CC/CC}$ and *Twist1*$^{CC/-}$ forelimb buds were smaller along the anteroposterior axis, and tapered distally compared to controls. Subsequently at E11.5 they were narrowed and curved anteriorly (Fig. S3A). By E12.5, the anterior mesenchyme had expanded significantly, although more in *Twist1*$^{CC/CC}$ than *Twist1*$^{CC/-}$ limbs, and curved dramatically anteriorly while the zeugopod remained narrow (Fig. S3A,C). Hindlimb buds resembled forelimb buds, displaying an almost 90 degree turn towards the anterior by E12.5 (Fig. S3A,C).

Molecular analyses of signaling center marker expression revealed that prior to substantial limb outgrowth, from 20 to 25 somite stages, the anteroposterior extent of *Fgf8* expression in the AER was reduced (Figs. 4Af,k). As forelimb outgrowth proceeded, this progressed into an absence of posterior *Fgf8* expression (Figs. 4Ag,l). As the autopod curved anteriorly, *Fgf8* expression expanded anteriorly (Figs. 4Ah,m). In the hindlimb the early absence of posterior expression was less pronounced (Figs. 4Ai,n), but the anterior *Fgf8* boundary expanded and persisted longer than normal (Figs. 4Aj,o).

Shh expression in the mutant embryos was dynamic (Fig. 4B). Early forelimb bud expression shifted distally, compared to normal posterior mesenchyme expression, and *Shh*+ cells were slightly dispersed (Figs. 4Ba,g). In early hindlimbs, expression was slightly elevated, and possibly anteriorly shifted, but not as severely as in mutant forelimbs (Figs. 4Bi,n). *Shh* expression then shifted to the posterior margin of the narrow, tapered limb buds (Figs. 4Bl,o). As the autopod expanded, an additional anterior *Shh* domain appeared. This domain was very robust in mutant forelimbs, but weak in mutant hindlimbs (Figs. 4Bh,f,m,p). Thus *Twist1* compound mutants display complex multiphasic changes in gene expression, with posterior effects followed by anterior ones.

FGF signaling is reduced in *Twist1* mutant limbs

The early reduction in the size of the *Fgf8* expression domain in the AER suggested that overall FGF signaling might be reduced in the *Twist1*^{CC} compound mutants. This would be consistent with previous reports that *Fgfr1* expression was severely reduced in *Twist1*$^{-/-}$ mesenchyme (O'Rourke et al., 2002; Zuniga et al., 2002). We therefore examined expression of *Fgfr1*, and the FGF targets *Spry1* (Mason et al., 2006) and *Etv5* (Mao et al., 2009; Zhang et al., 2009). *Fgfr1* expression was reduced, but present, in both forelimb and hindlimb mutant mesenchyme (Fig. 5A). *Spry1* was expressed in the subridge mesenchyme in wild type limbs, but was absent from posterior mesenchyme and reduced anteriorly and distally in mutant limbs (Fig. 5A). Similarly, *Etv5* expression was reduced, most strongly in forelimb posterior mesenchyme. Thus there is reduced but active FGF signaling in much of the *Twist1* compound mutant mesenchyme.

It is striking that there is no *Shh* expression in the posterior of mutant forelimb buds, even though there is posterior *Fgfr1* expression. While it is known that FGF signals are required for Shh expression, it is unclear whether *Shh* is induced autonomously in cells that transduce the FGF signal, or if FGF-dependent secondary signals are required. If Shh is induced autonomously, then the lack of *Fgf8* expression in the overlying posterior ectoderm might explain the lack of posterior *Shh* expression. To test how directly *Shh* is induced, we infected small groups of cells in chick limb buds with a replication defective virus expressing constitutively active Fgfr1 (Fgfr1*(Liu et al., 2001)) and assayed for *Shh* expression in infected

cells. Sections were processed sequentially by in situ hybridization for *Spry1* or *Shh* expression, then immunostained for retroviral gag expression to identify infected cells. The Fgfr1* virus induced *Spry1* expression in anterior, central and posterior limb mesenchyme, whereas it induced *Shh* expression only near the posterior margin (Fig. 5B). This restriction is consistent with other observations that the competence for *Shh* expression is limited to posterior mesenchyme by additional inputs that include both cell-autonomous transcription factors and non-autonomous signals from the overlying ectoderm (Zeller et al., 2009). In image overlays comparing the distribution of infected cells with the induced mRNA, there was excellent concordance between retroviral infection and induced patches of either *Spry1* or *Shh* mRNA (Fig. 5B, Fig. S4A,B). In some experiments the posterior AER was removed prior to infection to eliminate the major endogenous source of posterior FGF activity (Laufer et al., 1994), and *Shh* expression was still detected in some infected cells (Fig. S4C). These data provide evidence that *Shh*, like *Spry1*, is expressed by cells that receive FGF signals. While these data imply that no intermediary signal downstream of FGF is involved, they do not obviate the need for additional factors to impart competence for *Shh* expression to limb mesenchymal cells.

Twist1 regulates transcription factor expression

Null mutant mice for other transcription factors, notably within the Pax and Alx gene families, have limb and girdle cartilage phenotypes similar to the *Twist1*^{CC} mutants (Balling et al., 1988; Kuijper et al., 2005). While none is as severe as the *Twist1*^{CC} mutant phenotype, together they share many aspects, including preaxial polydactyly, anterior element aplasia and girdle defects. Previous reports showed that several of the genes are downregulated in *Twist1*$^{-/-}$ mutants. *Pax1*, which is required for scapula development, was also significantly reduced in *Twist1*^{CC} mutants (Fig. 6A,Fig. S3). We also found that *Alx4*, which is normally expressed in anterior limb mesenchyme, is markedly reduced in forelimb buds of *Twist1*^{CC} mutants, but is affected only mildly if at all in hindlimb buds (Fig. 6B,Fig. S3). These results are consistent with the idea that at least part of the *Twist1*^{CC} phenotype is due to misregulation of a network of downstream transcription factors.

We next examined whether the expression boundaries of genes implicated in positioning *Shh* expression in the early limb bud, *Tbx2*, *Tbx3* and *Hand2* (Davenport et al., 2003; te Welscher et al., 2002), might be altered in *Twist1*^{CC} mutants. As *Shh* expression is initiated, *Tbx3* and *Hand2* are expressed in approximately the posterior one-third of normal forelimb buds. In *Twist1*$^{CC/-}$ forelimbs both the *Tbx3* and *Hand2* expression boundaries are apparently unaffected through the 27 somite stage, prior to the onset of *Shh* expression (Fig. 6E,F). These borders do, however, shift anteriorly after *Shh* expression is initiated (Fig. 6E,F). The anterior expression border of *Tbx2* is also extended anteriorly in the *Twist1*^{CC} mutants after *Shh* expression begins (Fig. 6D). As each of these genes is responsive to Shh signaling (Lu et al., 2009), these changes are likely secondary to the shifting of the *Shh* expression domain.

We also asked whether expression of more downstream effectors of limb patterning, such as HoxA or HoxD cluster genes was normal in *Twist1*^{CC} mutants. *HoxD11*, which is normally expressed in posterior and distal limb mesenchyme, is expressed ectopically in anterior proximal forelimb and hindlimb buds of E10.5 *Twist1*^{CC} compound mutant embryos (Fig. 6C, Fig. S3). By contrast *HoxA11* is expressed normally in a zeugopodal domain in the mutants (Fig. S3). These results are consistent with posteriorization of the anterior mesenchyme, but normal proximodostal specification of the zeugopod.

Twist1 interacts genetically with Etv genes

Our molecular analyses and previous studies highlight the interaction of *Twist1* function with FGF signaling. Interestingly, we detect ectopic anterior *Shh* expression concomitant with reduced *Etv5* expression, which was recently identified as a negative regulator of anterior and

distal limb *Shh* expression downstream of FGF signaling (Mao et al., 2009; Zhang et al., 2009). Thus Twist1 and Etv genes might function in the same genetic pathway. To test this, we crossed *Twist1*$^{CC/+}$ mice with *Etv4* and *Etv5* null mutant mice (Livet et al., 2002; Lu et al., 2009) to progressively reduce Etv gene dosage, as *Etv4* and *Etv5* have overlapping functions (Lu et al., 2009; Mao et al., 2009; Zhang et al., 2009). Mice carrying up to two *Etv4* null alleles, one *Etv5* null allele and one *Twist1*^{CC} allele were viable, and their limb and girdle phenotypes were scored between E17.5 and P14.

Reducing Etv gene dosage had a dramatic effect on the distal forelimb skeleton (Fig. 7, Fig. S5; Table 2). Phenotypes ranged from simple preaxial polydactyly in 17% of *Etv4*$^{+/-}$;*Twist1*$^{CC/+}$ or *Etv5*$^{+/-}$;*Twist1*$^{CC/+}$ limbs, to radial aplasia and polydactyly with up to 7 forelimb digits in *Etv4*$^{-/-}$;*Etv5*$^{+/-}$;*Twist1*$^{CC/+}$ limbs (Fig. 7U,V; Table 2). Hindlimb phenotypes were also enhanced, with the strongest phenotypes including tibial aplasia and polydactyly (Fig. 7W,X). Strikingly we did not observe any defects in more proximal limb elements or the girdles. Removing up to 3 copies of the Etv genes in the context of two wild type *Twist1* alleles had almost no effect on skeletal pattern. The only limb defect we observed was a small preaxial cartilage digit that formed in one forelimb of a *Etv4*$^{-/-}$;*Etv5*$^{+/-}$ pup (Fig. 7F). These data provide evidence of strong dosage-sensitive interactions between *Twist1* and Etv genes to pattern the more distal limb skeleton.

Discussion

Previous studies aimed at understanding the role of Twist1 during limb development have been hampered by impaired limb bud outgrowth and early embryonic lethality of *Twist1*$^{-/-}$ embryos (Chen and Behringer, 1995; O'Rourke et al., 2002; Zuniga et al., 2002). Using an array of *Twist1* mutant alleles we generated an allelic series, which reveals that Twist1 has a range of previously unidentified roles in limb and limb girdle development. We demonstrate that Twist1 regulates limb signaling center function through precise positioning of the ZPA and both inhibition and maintenance of *Shh* expression, as well as influencing the anterior-posterior extent of the AER. Furthermore, we provide evidence that Twist1 acts through a gene network that includes *Hand2* and members of the Etv and aristaless families. Unexpectedly, we find that anterior limb skeletal morphology is most strongly affected despite severe defects in the posterior of Twist1 mutant limb buds. We present a model whereby discrete thresholds of Twist1 activity contribute to early limb bud patterning, and suggest how particular combinations of skeletal defects result from differing Twist1 levels.

Our results implicate Twist1 activity as critical for repressing, positioning and maintaining *Shh* expression in the developing limb bud. Progressively reducing Twist1 activity, as in the transition from *Twist1*$^{CC/+}$ to *Twist1*$^{CC/-}$ embryos, leads to progressively increasing amounts of ectopic *Shh* expression in the anterior of the bud. An anterior *Shh* domain was previously observed at low frequency in *Twist1*$^{+/-}$ hindlimbs (Bourgeois et al., 1998). *Twist1*$^{CC/+}$ hindlimbs display ectopic *Shh* expression and preaxial polydactyly at higher frequency, which is suppressed by reducing either *Shh* or *Hand2* dosage. *Hand2* is expressed strongly in posterior limb mesenchyme, and is required for *Shh* expression (Charite et al., 2000). The ectopic *Shh* expression we observe in *Twist1* mutants initiates at the far anterior margin of the limb bud, yet it is extremely sensitive to *Hand2* activity. This raises the question of how *Hand2* might act at such a long range. One possibility is that the small, weak domain of *Hand2* expressed at the base of the anterior autopod mediates this activity; perhaps this level of *Hand2* expression is normally insufficient to promote *Shh* expression, but can do so if Twist1 activity is modestly reduced.

There are interesting differences between the consequences of substantially reducing and completely removing Twist1 activity. In *Twist1*$^{CC/CC}$ or *Twist1*$^{CC/-}$ forelimb and hindlimb

buds, there is a large ectopic *Shh* domain. This was unexpected, as there is no ectopic domain in *Twist1*$^{-/-}$ limb buds. One possible explanation for this is that null mutants die before ectopic *Shh* expression is initiated. However we have observed ectopic *Shh* as early as e10.0 in *Twist1*$^{CC/-}$ forelimbs, when null embryos are viable (Chen and Behringer, 1995). Thus there is a sharp threshold of Twist1 activity that can support anterior *Shh* expression. Another activity threshold is apparent in the posterior of *Twist1*$^{CC/CC}$ or *Twist1*$^{CC/-}$ limbs, where reducing Twist1 activity shifts the normal *Shh* domain anteriorly and distally and expression is robust. A similar shift occurs in *Twist1*$^{-/-}$ embryos, however there *Shh* expression is weak (O'Rourke et al., 2002; Zuniga et al., 2002). This shift might be caused by anteriorly repositioning the field of cells competent to express *Shh*. Interestingly we found that the expression of positive factors such as *Hand2* did not shift prior to the onset of *Shh* expression, which suggests that *Twist1* is acting more directly as an inhibitor of *Shh* expression.

These changes in *Shh* expression can be attributed at least in part to alterations in FGF signaling from the AER to the underlying mesenchyme. Previous studies established that *Twist1* expression is downstream of FGF signaling from the AER, and is also required to maintain FGF receptor expression in the limb mesenchyme (Isaac et al., 2000; O'Rourke et al., 2002; Zuniga et al., 2002). Consistent with these results, we find that partial reductions in Twist1 activity lead to reduced FGF receptor expression and FGF pathway activity. There is also a secondary breakdown in signaling from the limb mesenchyme to the ectoderm that leads to a reduced AER, even before *Shh* expression is initiated. We also found that *Shh* expression is apparently induced autonomously in cells that receive FGF signals, without requiring a secondary signal downstream of FGF. This contrasts with the reciprocal signaling pathway from Shh to the overlying AER, which involves intermediary Gremlin antagonism of BMP activity (Zeller et al., 2009). Thus in *Twist1* mutants the anterior shift of the posterior AER border and reduced levels of FGF signaling activity together likely contribute to the anterior shift in the posterior *Shh* domain.

Recent studies also implicate FGF signaling as a major antagonist of *Shh* expression in anterior limb mesenchyme, with a critical role played by FGF targets of the Etv gene family (Mao et al., 2009; Zhang et al., 2009). Consistent with these observations Etv gene expression is lower when Twist1 activity is strongly reduced. By contrast in Etv conditional mutant limbs, *Twist1* expression and FGF signaling activity are unaffected, suggesting that Etv function lies downstream and possibly parallel to that of Twist1 (Zhang et al., 2009). We find that *Twist1*$^{CC/+}$;Etv mutant combinations cause preaxial polydactyly plus anterior zeugopod defects, each of which we detect in *Twist1*$^{CC/CC}$ or *Twist1*$^{CC/-}$ mutants. This synergistic interaction provides strong evidence in support of Etv genes mediating Twist1 activity. However in Etv mutants, the zeugopod is either unaffected, or both elements are modestly reduced (Mao et al., 2009; Zhang et al., 2009). Furthermore in *Twist1* mutants we observe as few as three digits in the forelimb autopod, consistent with a shortened AER, while Etv mutants have a normal or extended AER and do not have reduced digit numbers (Mao et al., 2009; Zhang et al., 2009). Thus changes in Etv activity account for only part of the *Twist1* mutant phenotype.

Our results and previous observations show that Twist1 is required for the expression of *Alx3* and *Alx4*, members of the aristaless gene family (O'Rourke et al., 2002). Twist1 might be required for expression of another family member, *Cart1*, but we were unable to detect any obvious differences in *Cart1* expression in Twist1 mutants (not shown), because *Cart1* is at low levels in the limb mesenchyme (Beverdam and Meijlink, 2001). Single and compound loss-of-function mutants for *Alx4*, *Alx3* and *Cart1* cause progressive limb phenotypes that overlap with the progression of *Twist1* mutant phenotypes. These range from weak preaxial polydactyly and missing deltoid tuberosities in single mutants to extreme polydactyly with tibial hypoplasia or aplasia in compound mutants (Beverdam et al., 2001; Qu et al., 1999).

They can also exhibit shortened clavicles, abnormal scapulas, and missing or hypoplastic pubic bones (Kuijper et al., 2005). Thus changes in aristaless-family gene activity might contribute to both limb and girdle aspects of the *Twist1* mutant phenotype.

Interestingly aristaless gene expression is dependent on Twist1 primarily in the forelimb. While expansion of *Hand2* into the anterior limb can repress *Alx4* expression, we detect loss of *Alx4* expression prior to any shift in *Hand2* expression. This suggests that *Shh* derepression in *Twist1* mutant forelimbs is affected by both aristaless and Etv activity, while in hindlimbs it is due mostly to reduced Etv function. This would be consistent with the relatively stronger skeletal phenotypes such as the ulnar duplications in *Twist1* mutant forelimbs.

While Twist1 clearly modulates Shh expression and FGF signaling from the AER, its activity is not restricted to this distal mesenchyme patterning system. The limb girdles develop independent of the ZPA or AER, as neither pelvis nor scapula is affected in $Shh^{-/-}$ or $Fgf4^{-/-};Fgf8^{-/-}$ mutant animals (Boulet et al., 2004; Chiang et al., 2001; Sun et al., 2002). Furthermore the antagonism between Hand2 and Twist1 is not unique to distal limb mesenchyme, as the Twist1 pubic bone and clavicle defects are sensitive to *Hand2* dosage.

Our studies show that Twist1 levels are critically important for exerting different aspects of its function (Fig. 8). High Twist1 activity is required to repress *Shh* expression in the anterior limb bud, primarily through FGF signaling and Etv function and secondarily via aristaless gene activity. It also involves competitive antagonism with Hand2. Thus in limbs with only modestly reduced Twist1 activity, such as in $Twist1^{CC/+}$ embryos, a late domain of ectopic *Shh* expression induces weak preaxial polydactyly.

In $Twist1^{CC/CC}$ or $Twist1^{CC/-}$ embryos that have less Twist1 activity, the molecular defects are more severe. Prior to the onset of *Shh* expression the anterior-posterior extent of the AER is reduced. This leads to an anterior shift in the strongest region of FGF signaling, and reduction in the antagonistic activity between Twist1/Etv and Hand2, thereby resulting in an anterior shift in initial *Shh* expression. Furthermore because the AER is smaller, the most posterior (and probably anterior) limb mesenchyme regions have reduced outgrowth. There might be increased apoptosis in posterior mesenchyme, as occurs in Twist1 null limb buds (O'Rourke et al., 2002; Zuniga et al., 2002), although we have not consistently detected this in $Twist1^{CC/CC}$ or $Twist1^{CC/-}$ limb buds (not shown). As the limb grows out, the *Shh* domain becomes restricted to the posterior margin of the now smaller bud. Subsequently on the anterior, there is earlier *Shh* derepression. This anterior *Shh* domain then rescues and extends the anterior AER, expanding the distal limb bud.

The morphological consequences of these changes reflect both the degree of AER contraction and the timing of anterior *Shh* expression. In $Twist1^{CC/CC}$ limbs the most pronounced early signaling defects are on the posterior, yet only the anterior zeugopodal elements are affected. This is probably because when the limb bud narrows, the zeugopodal primordium supports formation of only one cartilage condensation, and as the *Shh* domain is strong and nearby, this tissue is specified as posterior. Consistent with this idea, fate-mapping experiments reveal a Shh-response only in posterior zeugopod (Harfe et al., 2004). If Twist1 activity is further reduced, as in $Twist1^{CC/-}$ limbs, then initial outgrowth is more severely compromised but is rescued by more robust and earlier ectopic *Shh* as well as rescue of the overlying AER. This expands the zeugopodal precursor region sufficiently to support two condensations, both of which will be specified as posterior. However this rescue occurs too late to promote normal stylopod development. This mechanism would account for both the hypoplastic humerus and duplicated ulna found in $Twist1^{CC/-}$ forelimbs. Interestingly in these animals the hindlimbs have a normal femur, and no duplication of the fibula, although the tibia and autopod are

severely affected. This might reflect the minimal change in *Alx4* expression in the anterior hindlimb bud.

Shh expression in the limb is controlled by a conserved enhancer element that is required for expression in the posterior limb bud (Ros et al., 2003; Sagai et al., 2005), but that when mutated can also direct expression to the limb anterior (Sagai et al., 2004; Sharpe et al., 1999). The protein complexes that interact with this element are not yet well defined (Amano et al., 2009). But as *Twist1*, *Hand2*, Etv and aristaless family genes all encode transcription factors, they might directly regulate this enhancer element. Furthermore, these proteins have the potential to interact physically as well as genetically. Physical interaction between Twist1 and Hand2 is already well documented, and their choice of binding partners is critical for in vivo function (Barnes and Firulli, 2009; Firulli et al., 2005; Firulli et al., 2007). It will be interesting to learn whether proteins of these other families bind to Twist1 or Hand2, or if they act less directly to mediate Twist1 regulation of *Shh* expression, and ultimately limb development.

Supplementary Material

Refer to Web version on PubMed Central for supplementary material.

Acknowledgments

We thank Alex Paul, Amy Daniel, Shannon Giorgianni for experimental support, and Andreas Kottmann, Cliff Tabin, Peter Cserjesi and Monica Justice for mice. Funding was provided by the NIH (R01-HD30284 to RRB, R01-DK075578 to FC, F31-DE1453 to DK, P30-AR044535 and R01-DK081515 to EL) and March of Dimes (5-FY99-855 to EL).

References

Amano T, Sagai T, Tanabe H, Mizushina Y, Nakazawa H, Shiroishi T. Chromosomal dynamics at the Shh locus: limb bud-specific differential regulation of competence and active transcription. Dev Cell 2009;16:47–57. [PubMed: 19097946]

Balling R, Deutsch U, Gruss P. undulated, a mutation affecting the development of the mouse skeleton, has a point mutation in the paired box of Pax 1. Cell 1988;55:531–535. [PubMed: 3180219]

Barnes RM, Firulli AB. A twist of insight - the role of Twist-family bHLH factors in development. Int J Dev Biol 2009;53:909–924. [PubMed: 19378251]

Beverdam A, Brouwer A, Reijnen M, Korving J, Meijlink F. Severe nasal clefting and abnormal embryonic apoptosis in Alx3/Alx4 double mutant mice. Development 2001;128:3975–3986. [PubMed: 11641221]

Beverdam A, Meijlink F. Expression patterns of group-I aristaless-related genes during craniofacial and limb development. Mech Dev 2001;107:163–167. [PubMed: 11520673]

Bialek P, Kern B, Yang X, Schrock M, Sosic D, Hong N, Wu H, Yu K, Ornitz DM, Olson EN, Justice MJ, Karsenty G. A twist code determines the onset of osteoblast differentiation. Dev Cell 2004;6:423–435. [PubMed: 15030764]

Boulet AM, Moon AM, Arenkiel BR, Capecchi MR. The roles of Fgf4 and Fgf8 in limb bud initiation and outgrowth. Dev Biol 2004;273:361–372. [PubMed: 15328019]

Bourgeois P, Bolcato-Bellemin AL, Danse JM, Bloch-Zupan A, Yoshiba K, Stoetzel C, Perrin-Schmitt F. The variable expressivity and incomplete penetrance of the twist-null heterozygous mouse phenotype resemble those of human Saethre-Chotzen syndrome. Hum Mol Genet 1998;7:945–957. [PubMed: 9580658]

Burke AC, Nelson CE, Morgan BA, Tabin C. Hox genes and the evolution of vertebrate axial morphology. Development 1995;121:333–346. [PubMed: 7768176]

Cai J, Jabs EW. A twisted hand: bHLH protein phosphorylation and dimerization regulate limb development. Bioessays 2005;27:1102–1106. [PubMed: 16237669]

Chapman DL, Garvey N, Hancock S, Alexiou M, Agulnik SI, Gibson-Brown JJ, Cebra-Thomas J, Bollag RJ, Silver LM, Papaioannou VE. Expression of the T-box family genes, Tbx1-Tbx5, during early mouse development. Dev Dyn 1996;206:379–390. [PubMed: 8853987]

Charite J, McFadden DG, Olson EN. The bHLH transcription factor dHAND controls Sonic hedgehog expression and establishment of the zone of polarizing activity during limb development. Development 2000;127:2461–2470. [PubMed: 10804186]

Chen YT, Akinwunmi PO, Deng JM, Tam OH, Behringer RR. Generation of a Twist1 conditional null allele in the mouse. Genesis 2007;45:588–592. [PubMed: 17868088]

Chen ZF, Behringer RR. Twist is required in head mesenchyme for cranial neural tube morphogenesis. Genes Dev 1995;9:686–699. [PubMed: 7729687]

Chiang C, Litingtung Y, Harris MP, Simandl BK, Li Y, Beachy PA, Fallon JF. Manifestation of the limb prepattern: limb development in the absence of sonic hedgehog function. Dev Biol 2001;236:421–435. [PubMed: 11476582]

Chotteau-Lelievre A, Dolle P, Peronne V, Coutte L, de Launoit Y, Desbiens X. Expression patterns of the Ets transcription factors from the PEA3 group during early stages of mouse development. Mech Dev 2001;108:191–195. [PubMed: 11578874]

Crossley PH, Martin GR. The mouse Fgf8 gene encodes a family of polypeptides and is expressed in regions that direct outgrowth and patterning in the developing embryo. Development 1995;121:439–451. [PubMed: 7768185]

Davenport TG, Jerome-Majewska LA, Papaioannou VE. Mammary gland, limb and yolk sac defects in mice lacking Tbx3, the gene mutated in human ulnar mammary syndrome. Development 2003;130:2263–2273. [PubMed: 12668638]

Davis AP, Witte DP, Hsieh-Li HM, Potter SS, Capecchi MR. Absence of radius and ulna in mice lacking hoxa-11 and hoxd-11. Nature 1995;375:791–795. [PubMed: 7596412]

Fallon JF, Lopez A, Ros MA, Savage MP, Olwin BB, Simandl BK. FGF-2: apical ectodermal ridge growth signal for chick limb development. Science 1994;264:104–107. [PubMed: 7908145]

Fernandez-Teran M, Piedra ME, Kathiriya IS, Srivastava D, Rodriguez-Rey JC, Ros MA. Role of dHAND in the anterior-posterior polarization of the limb bud: implications for the Sonic hedgehog pathway. Development 2000;127:2133–2142. [PubMed: 10769237]

Firulli BA, Krawchuk D, Centonze VE, Vargesson N, Virshup DM, Conway SJ, Cserjesi P, Laufer E, Firulli AB. Altered Twist1 and Hand2 dimerization is associated with Saethre-Chotzen syndrome and limb abnormalities. Nat Genet 2005;37:373–381. [PubMed: 15735646]

Firulli BA, Redick BA, Conway SJ, Firulli AB. Mutations within helix I of Twist1 result in distinct limb defects and variation of DNA binding affinities. J Biol Chem 2007;282:27536–27546. [PubMed: 17652084]

Hamburger V, Hamilton HL. A series of normal stages in the development of the chick embryo. J Exp Morph 1951;88:49–92.

Harfe BD, Scherz PJ, Nissim S, Tian H, McMahon AP, Tabin CJ. Evidence for an expansion-based temporal Shh gradient in specifying vertebrate digit identities. Cell 2004;118:517–528. [PubMed: 15315763]

Hui CC, Slusarski D, Platt KA, Holmgren R, Joyner AL. Expression of three mouse homologs of the Drosophila segment polarity gene cubitus interruptus, Gli, Gli-2, and Gli-3, in ectoderm- and mesoderm-derived tissues suggests multiple roles during postimplantation development. Dev Biol 1994;162:402–413. [PubMed: 8150204]

Isaac A, Cohn MJ, Ashby P, Ataliotis P, Spicer DB, Cooke J, Tickle C. FGF and genes encoding transcription factors in early limb specification. Mech Dev 2000;93:41–48. [PubMed: 10781938]

Jeong J, Mao J, Tenzen T, Kottmann AH, McMahon AP. Hedgehog signaling in the neural crest cells regulates the patterning and growth of facial primordia. Genes Dev 2004;18:937–951. [PubMed: 15107405]

Kuijper S, Beverdam A, Kroon C, Brouwer A, Candille S, Barsh G, Meijlink F. Genetics of shoulder girdle formation: roles of Tbx15 and aristaless-like genes. Development 2005;132:1601–1610. [PubMed: 15728667]

Laufer E, Dahn R, Orozco OE, Yeo CY, Pisenti J, Henrique D, Abbott UK, Fallon JF, Tabin C. Expression of Radical fringe in limb-bud ectoderm regulates apical ectodermal ridge formation. Nature 1997;386:366–373. [PubMed: 9121552]

Laufer E, Nelson CE, Johnson RL, Morgan BA, Tabin C. Sonic hedgehog and Fgf-4 act through a signaling cascade and feedback loop to integrate growth and patterning of the developing limb bud. Cell 1994;79:993–1003. [PubMed: 8001146]

Liu JP, Laufer E, Jessell TM. Assigning the positional identity of spinal motor neurons: rostrocaudal patterning of Hox-c expression by FGFs, Gdf11, and retinoids. Neuron 2001;32:997–1012. [PubMed: 11754833]

Livet J, Sigrist M, Stroebel S, De Paola V, Price SR, Henderson CE, Jessell TM, Arber S. ETS gene Pea3 controls the central position and terminal arborization of specific motor neuron pools. Neuron 2002;35:877–892. [PubMed: 12372283]

Loebel DA, O'Rourke MP, Steiner KA, Banyer J, Tam PP. Isolation of differentially expressed genes from wild-type and Twist mutant mouse limb buds. Genesis 2002;33:103–113. [PubMed: 12124942]

Logan M, Martin JF, Nagy A, Lobe C, Olson EN, Tabin CJ. Expression of Cre Recombinase in the developing mouse limb bud driven by a Prxl enhancer. Genesis 2002;33:77–80. [PubMed: 12112875]

Lu BC, Cebrian C, Chi X, Kuure S, Kuo R, Bates CM, Arber S, Hassell J, MacNeil L, Hoshi M, Jain S, Asai N, Takahashi M, Schmidt-Ott KM, Barasch J, D'Agati V, Costantini F. Etv4 and Etv5 are required downstream of GDNF and Ret for kidney branching morphogenesis. Nat Genet 2009;41:1295–1302. [PubMed: 19898483]

Mao J, McGlinn E, Huang P, Tabin CJ, McMahon AP. Fgf-dependent Etv4/5 activity is required for posterior restriction of Sonic Hedgehog and promoting outgrowth of the vertebrate limb. Dev Cell 2009;16:600–606. [PubMed: 19386268]

Marigo V, Davey RA, Zuo Y, Cunningham JM, Tabin CJ. Biochemical evidence that patched is the Hedgehog receptor. Nature 1996;384:176–179. [PubMed: 8906794]

Mason JM, Morrison DJ, Basson MA, Licht JD. Sprouty proteins: multifaceted negative-feedback regulators of receptor tyrosine kinase signaling. Trends Cell Biol 2006;16:45–54. [PubMed: 16337795]

Minowada G, Jarvis LA, Chi CL, Neubuser A, Sun X, Hacohen N, Krasnow MA, Martin GR. Vertebrate Sprouty genes are induced by FGF signaling and can cause chondrodysplasia when overexpressed. Development 1999;126:4465–4475. [PubMed: 10498682]

Niswander L, Jeffrey S, Martin GR, Tickle C. A positive feedback loop coordinates growth and patterning in the vertebrate limb. Nature 1994;371:609–612. [PubMed: 7935794]

Niswander L, Tickle C, Vogel A, Booth I, Martin GR. FGF-4 replaces the apical ectodermal ridge and directs outgrowth and patterning of the limb. Cell 1993;75:579–587. [PubMed: 8221896]

O'Rourke MP, Soo K, Behringer RR, Hui CC, Tam PP. Twist plays an essential role in FGF and SHH signal transduction during mouse limb development. Dev Biol 2002;248:143–156. [PubMed: 12142027]

Patton JT, Kaufman MH. The timing of ossification of the limb bones, and growth rates of various long bones of the fore and hind limbs of the prenatal and early postnatal laboratory mouse. J Anat 1995;186 (Pt 1):175–185. [PubMed: 7649813]

Peters KG, Werner S, Chen G, Williams LT. Two FGF receptor genes are differentially expressed in epithelial and mesenchymal tissues during limb formation and organogenesis in the mouse. Development 1992;114:233–243. [PubMed: 1315677]

Qu S, Niswender KD, Ji Q, van der Meer R, Keeney D, Magnuson MA, Wisdom R. Polydactyly and ectopic ZPA formation in Alx-4 mutant mice. Development 1997;124:3999–4008. [PubMed: 9374397]

Qu S, Tucker SC, Zhao Q, deCrombrugghe B, Wisdom R. Physical and genetic interactions between Alx4 and Cart1. Development 1999;126:359–369. [PubMed: 9847249]

Riddle RD, Johnson RL, Laufer E, Tabin C. Sonic hedgehog mediates the polarizing activity of the ZPA. Cell 1993;75:1401–1416. [PubMed: 8269518]

Roelink H, Augsburger A, Heemskerk J, Korzh V, Norlin S, Ruiz i Altaba A, Tanabe Y, Placzek M, Edlund T, Jessell TM, et a. Floor plate and motor neuron induction by vhh-1, a vertebrate homolog of hedgehog expressed by the notochord. Cell 1994;76:761–775. [PubMed: 8124714]

Ros MA, Dahn RD, Fernandez-Teran M, Rashka K, Caruccio NC, Hasso SM, Bitgood JJ, Lancman JJ, Fallon JF. The chick oligozeugodactyly (ozd) mutant lacks sonic hedgehog function in the limb. Development 2003;130:527–537. [PubMed: 12490559]

Sagai T, Hosoya M, Mizushina Y, Tamura M, Shiroishi T. Elimination of a long-range cis-regulatory module causes complete loss of limb-specific Shh expression and truncation of the mouse limb. Development 2005;132:797–803. [PubMed: 15677727]

Sagai T, Masuya H, Tamura M, Shimizu K, Yada Y, Wakana S, Gondo Y, Noda T, Shiroishi T. Phylogenetic conservation of a limb-specific, cis-acting regulator of Sonic hedgehog (Shh). Mamm Genome 2004;15:23–34. [PubMed: 14727139]

Saunders J Jr. The proximo-distal sequence of origin of the parts of the chick wing and the role of the ectoderm. J Exp Zool 1948;108:363–403. [PubMed: 18882505]

Sharpe J, Lettice L, Hecksher-Sorensen J, Fox M, Hill R, Krumlauf R. Identification of sonic hedgehog as a candidate gene responsible for the polydactylous mouse mutant Sasquatch. Curr Biol 1999;9:97–100. [PubMed: 10021368]

Srivastava D, Cserjesi P, Olson EN. A subclass of bHLH proteins required for cardiac morphogenesis. Science 1995;270:1995–1999. [PubMed: 8533092]

Srivastava D, Thomas T, Lin Q, Kirby ML, Brown D, Olson EN. Regulation of cardiac mesodermal and neural crest development by the bHLH transcription factor, dHAND. Nat Genet 1997;16:154–160. [PubMed: 9171826]

Sun X, Mariani FV, Martin GR. Functions of FGF signalling from the apical ectodermal ridge in limb development. Nature 2002;418:501–508. [PubMed: 12152071]

te Welscher P, Fernandez-Teran M, Ros MA, Zeller R. Mutual genetic antagonism involving GLI3 and dHAND prepatterns the vertebrate limb bud mesenchyme prior to SHH signaling. Genes Dev 2002;16:421–426. [PubMed: 11850405]

Vargesson N, Luria V, Messina I, Erskine L, Laufer E. Expression patterns of Slit and Robo family members during vertebrate limb development. Mech Dev 2001;106:175–180. [PubMed: 11472852]

Webb GN, Byrd RA. Simultaneous differential staining of cartilage and bone in rodent fetuses: an alcian blue and alizarin red S procedure without glacial acetic acid. Biotech Histochem 1994;69:181–185. [PubMed: 7522588]

Zakany J, Kmita M, Duboule D. A dual role for Hox genes in limb anterior-posterior asymmetry. Science 2004;304:1669–1672. [PubMed: 15192229]

Zeller R, Lopez-Rios J, Zuniga A. Vertebrate limb bud development: moving towards integrative analysis of organogenesis. Nat Rev Genet 2009;10:845–858. [PubMed: 19920852]

Zhang S, Lin Y, Itaranta P, Yagi A, Vainio S. Expression of Sprouty genes 1, 2 and 4 during mouse organogenesis. Mech Dev 2001;109:367–370. [PubMed: 11731251]

Zhang Z, Verheyden JM, Hassell JA, Sun X. FGF-regulated Etv genes are essential for repressing Shh expression in mouse limb buds. Dev Cell 2009;16:607–613. [PubMed: 19386269]

Zuniga A, Quillet R, Perrin-Schmitt F, Zeller R. Mouse Twist is required for fibroblast growth factor-mediated epithelial-mesenchymal signalling and cell survival during limb morphogenesis. Mech Dev 2002;114:51–59. [PubMed: 12175489]

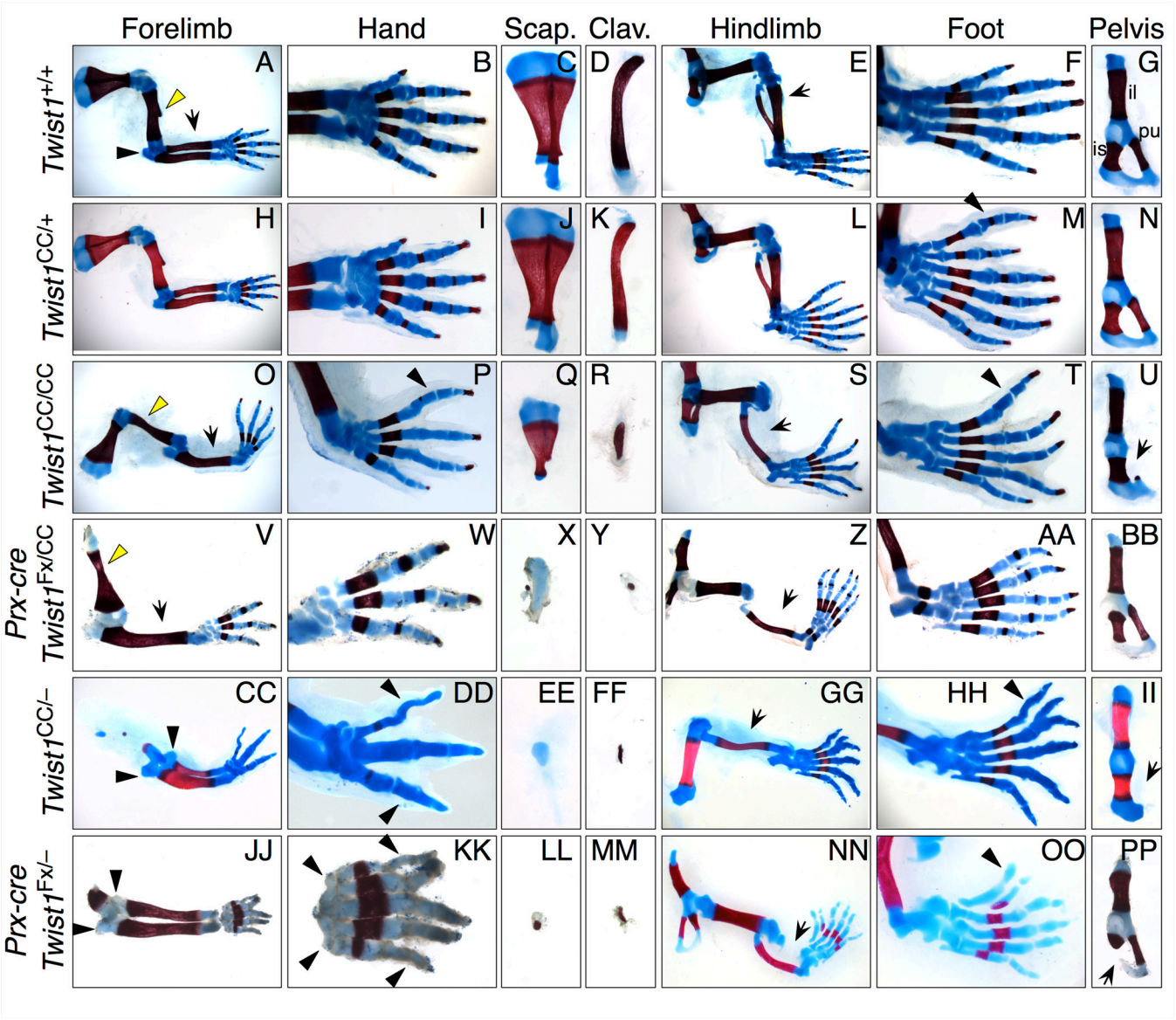

Figure 1. Limb and girdle skeletal phenotypes in *Twist1*^{CC} compound mutant mice

Skeletal preparations of E17.5-P2 limbs carrying combinations of *Twist1*^{CC}, *Twist1*$^{-}$, and *Twist1*^{Fx} alleles show progressively more severe limb and girdle defects.

(A–G) Wild type, cartilage (blue) and bone (red).

(H–N) *Twist1*$^{CC/+}$, hindlimb with preaxial polydactyly (M, arrowhead).

(O–U) *Twist1*$^{CC/CC}$, forelimb with radial aplasia and absent deltoid tuberosity (O, dt, arrow and arrowhead), absent anterior digit and AP mirror symmetry (P, arrowhead), reduced scapula (Q) and clavicle (R); hindlimb with tibial aplasia (S, arrow), disorganized AP digit pattern (T, arrowhead) and hypoplastic pubis (U, arrow).

(V-BB) *Prx1-cre*; *Twist1*$^{CC/Fx}$, forelimb with widened humerus and absent dt (V, arrowhead), radial aplasia (V, arrow), three digits (W) and severely hypoplastic scapula (X) and clavicle (Y); hindlimb with tibial aplasia (Z, arrow) and posteriorized AP digit pattern (AA).

(CC-II) *Twist1*$^{CC/-}$ forelimb with duplicated ulna and olecranon (CC, arrowheads), three digits in posteriorized mirror symmetric pattern (DD, arrowheads) and severely hypoplastic scapula

(EE) and clavicle (FF); hindlimb with tibial aplasia (GG, arrow), disrupted AP digit pattern (HH, arrowhead) with bifurcation, and absent pubis (II, arrow).
(JJ-PP) *Prx1-cre*; *Twist1*$^{Fx/-}$ forelimb with duplicated ulna and olecranon (JJ, arrowheads), five digits with striking mirror symmetry (KK, arrowheads), severely hypoplastic scapula (LL) and clavicle (MM); hindlimb with tibial aplasia (NN, arrow), preaxial polydactyly with disorganized cartilage elements (OO, arrowhead), and hypoplastic ischium (PP, arrow). Delays in ossification center formation due to reduced Twist1 activity were previously described (Bialek et al., 2004).
Scap: scapula, clav: clavicle, il: ilium, is: ischium, pu: pubis.

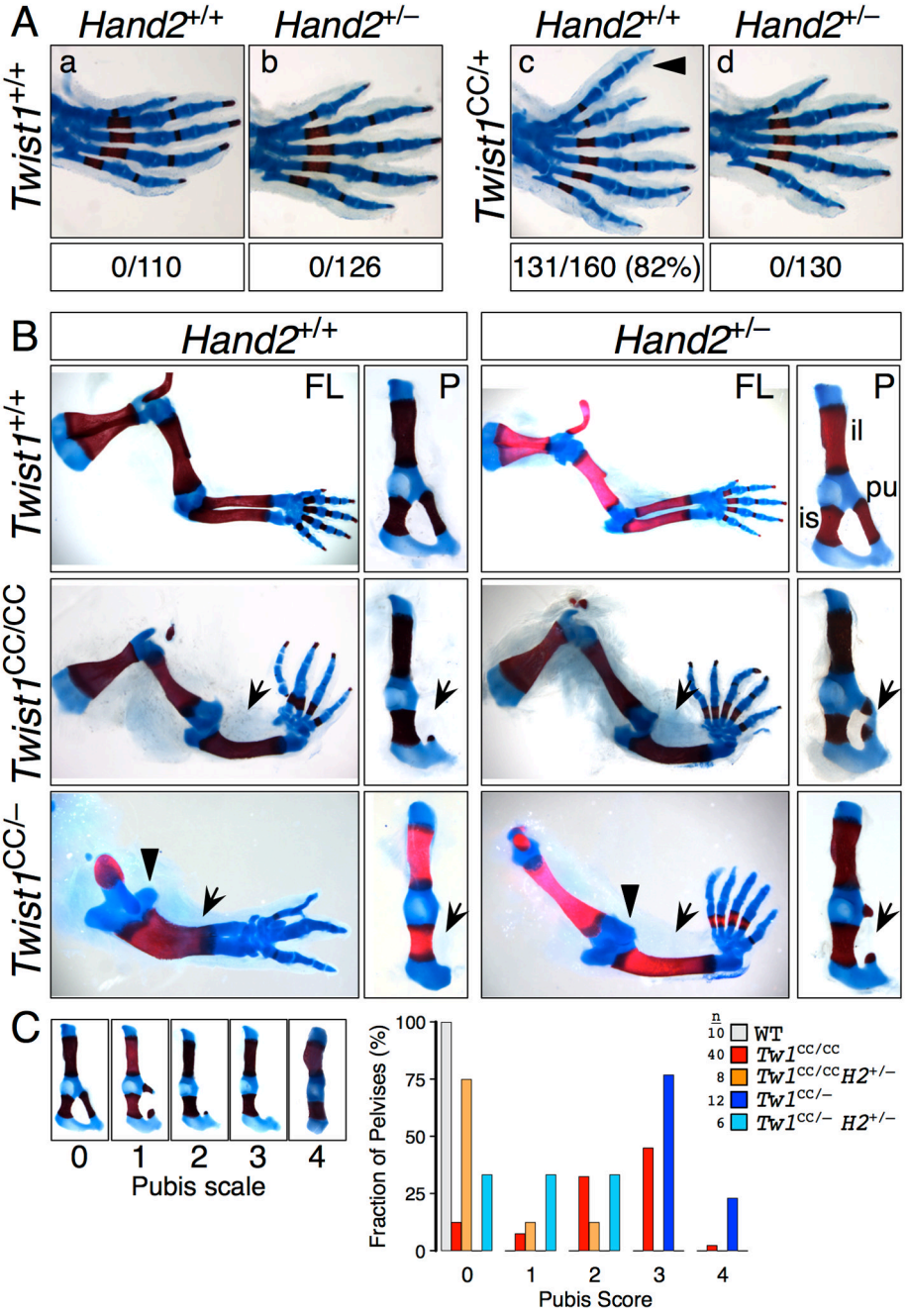

Figure 2. Genetic interactions between *Twist1*^{CC} and *Hand2*

(A) *Twist1*$^{CC/+}$ hindlimb polydactyly is sensitive to *Hand2* dosage. Hindlimbs of F1 progeny of *Twist1*$^{CC/+}$; *Hand2*$^{+/+}$ X *Twist1*$^{+/+}$; *Hand2*$^{+/–}$ intercross scored for preaxial polydactyly (arrowhead) show complete suppression of polydactyly in double heterozygotes ($p<0.001$, chi squared).

(B) *Twist1*^{CC} forelimb and pelvis phenotypes are sensitive to *Hand2* dosage. *Hand2* null allele was crossed onto compound *Twist1* genotypes as indicated. *Twist1*$^{CC/CC}$ limbs with reduced *Hand2* gene dosage (row 2) have less severe pubis hypoplasia (P columns, arrows) but still display radial aplasia (FL columns, arrows). *Twist1*$^{CC/–}$ limbs with reduced *Hand2* gene dosage (row 3) resemble less severe *Twist1*$^{CC/CC}$ limbs, with duplicated ulnae replaced by radial

aplasia (FL columns, arrows and arrowhead), increased digit number, and reduced severity of pubis hypoplasia (P columns, arrows). FL, forelimb; P, pelvis; il, ilium; pu, pubis; is, ischium. (C) *Twist1*^{CC} pubis defects were scored on a scale of increasing severity from 0 to 4 (left panels) and plotted as a percent fraction of total pelvises scored for each genotype. Reducing *Hand2* gene dosage in *Twist1*$^{CC/CC}$ or *Twist1*$^{CC/-}$ pelvises significantly shifts pubis scores to lesser values ($p<0.001$ for each, Mann-Whitney).

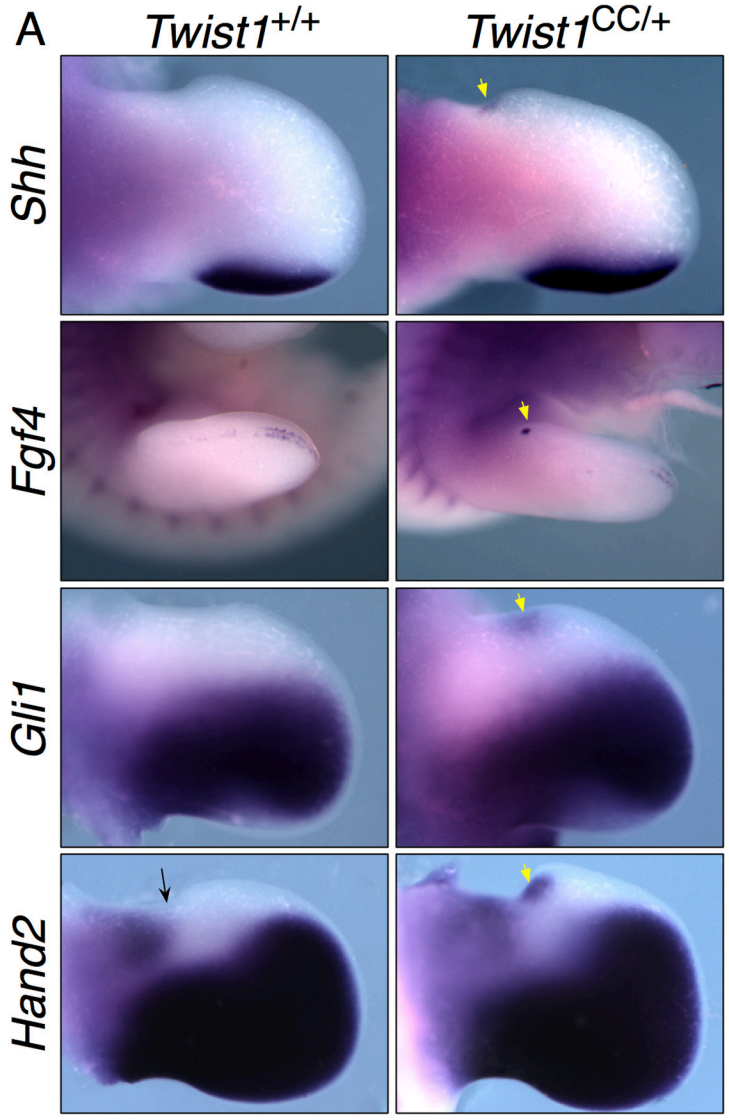

B $Twist1^{CC/+}$ X $Hand2^{+/-}$

	$Twist1^{CC/+}$	
	$Hand2^{+/+}$	$Hand2^{+/-}$
Shh	2/23 (7%)	0/8 (0%)
Fgf4	10/20 (50%)	0/7 (0%)
Gli1	31/42 (74%)	0/3 (0%)
Hand2	33/44 (75%)	0/9 (0%)

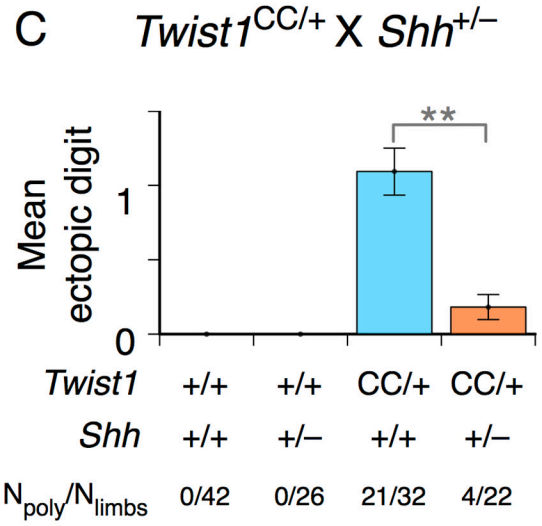

Figure 3. *Twist1* and *Hand2* activities in anterior limb bud converge at the regulation of *Shh* activity

(A) E11.5 $Twist1^{CC/+}$ hindlimb buds displaying ectopic anterior RNA expression of *Shh* and the *Shh* target genes *Fgf4*, *Gli1* and *Hand2* (white arrows). Note presence of proximal anterior *Hand2* domain (black arrow).

(B) Reducing *Hand2* gene dosage suppresses ectopic anterior gene expression in $Twist1^{CC/+}$ embryos. Frequency of ectopic anterior gene expression detected in E11.0 – E13.0 $Twist1^{CC/+}$; $Hand2^{+/+}$ and $Twist1^{CC/+}$; $Hand2^{+/-}$ hindlimbs (N=limbs with ectopic expression/limbs examined).

(C) $Twist1^{CC/+}$; $Shh^{+/-}$ progeny of $Twist1^{CC/+}$ X $Shh^{+/-}$ intercross show significantly reduced frequency and severity of hindlimb polydactyly, indicating the $Twist1^{CC/+}$hindlimb polydactyly is *Shh*-dependent. **: p<0.001. (N=limbs with polydactyly/limbs examined).

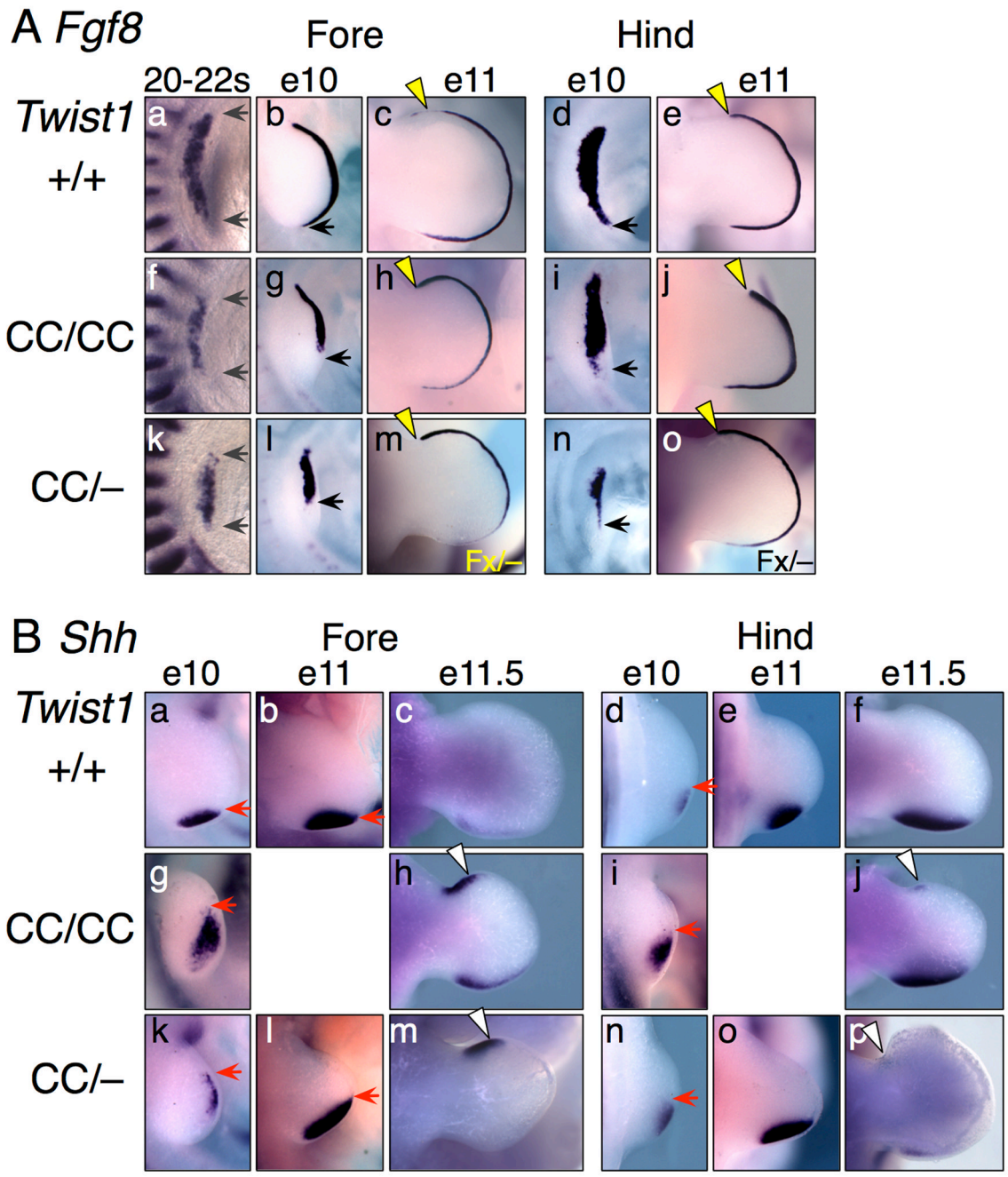

Figure 4. *Fgf8* and *Shh* expression defects in *Twist1* mutant limbs

(A) *Fgf8* RNA expression in whole-mount limb buds. At 20–22 somites, the AP length of *Fgf8* expression is significantly narrowed (gray arrows) in *Twist1*^{CC} mutant forelimb buds. At E10, posterior *Fgf8* expression is absent (forelimb) or reduced (hindlimb) in the small *Twist1*^{CC} mutant buds (black arrows). At E11 *Twist1*$^{CC/CC}$ and *Prx1-cre; Twist1*$^{Fx/–}$ (Fx/–; panels m,o) limb buds have increased anterior *Fgf8* expression extending to the anterior limb boundary (yellow arrowheads).

(B) *Shh* RNA expression in whole-mount limb buds. At E10, *Shh* expression is shifted anteriorly and distally (red arrows) and is less organized in *Twist1* mutant limb buds. By E11, *Shh* expression encompasses the entire posterior and distal regions of the small *Twist1*$^{CC/–}$

forelimb bud (red arrows), and encompasses much of the posterior region in hindlimb buds. Subsequently, at E11.5, a strong ectopic anterior *Shh* domain is detected in the mutant forelimbs, with a lesser ectopic domain in hindlimbs (white arrowheads).

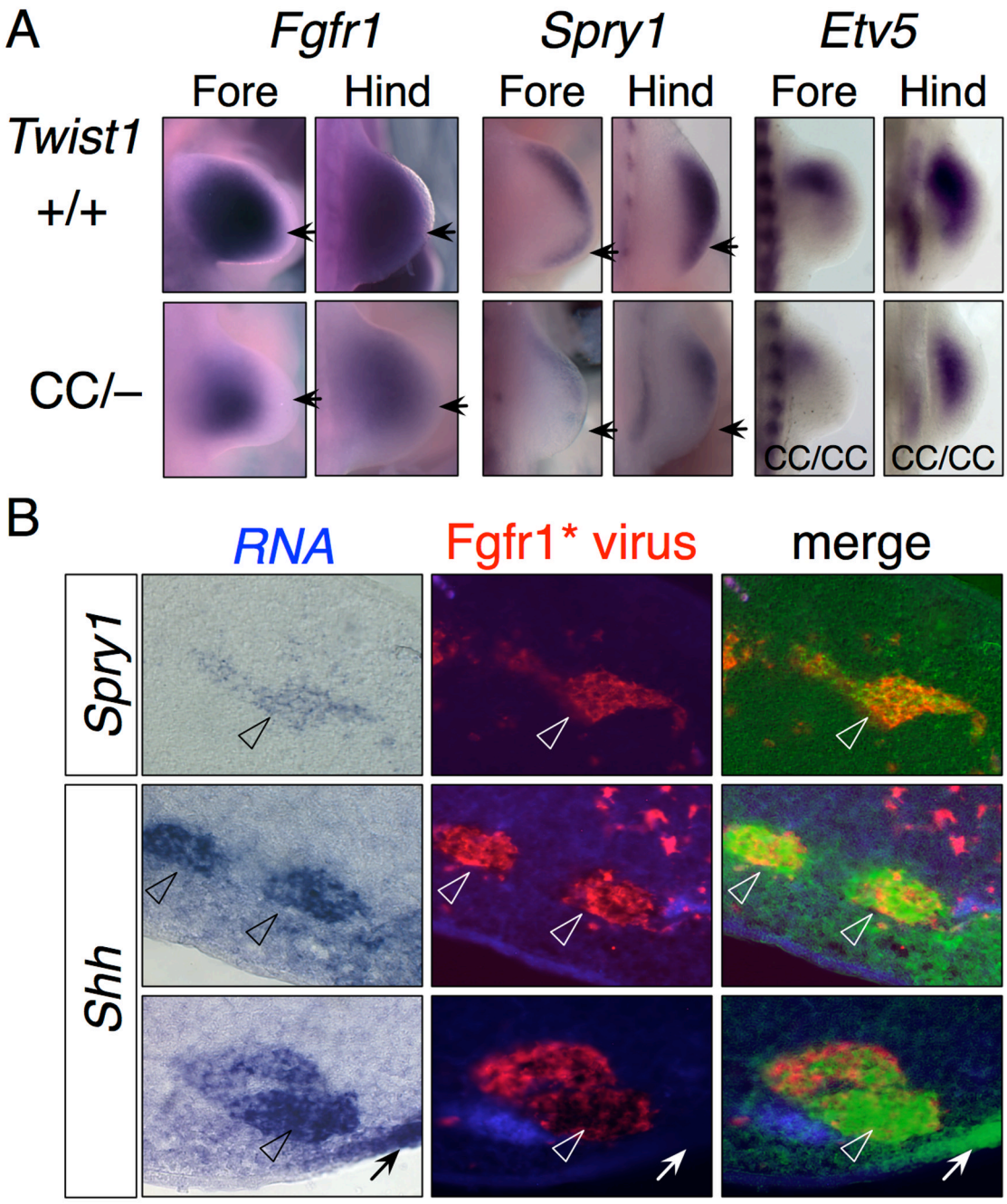

Figure 5. FGF signaling is compromised in *Twist1* mutants

(A) *Fgfr1* and *Spry1* expression in wild type and *Twist1*$^{CC/-}$ limb buds. *Fgfr1* expression is reduced but not absent in mutant limb buds, particularly in the distal and posterior margins (arrows). *Spry1* expression is substantially reduced in *Twist1*$^{CC/-}$ limb buds with less expression in the posterior (arrow), and overall expression in hindlimb higher than forelimb (arrow). *Etv5* expression is also significantly reduced in *Twist1*$^{CC/CC}$ limb buds.

(B) *Shh* is induced cell-autonomously by FGF signaling. Sections of limb buds infected at stage 20 with a replication-defective retrovirus expressing constitutively active *Fgfr1*, harvested 36 h post-infection, and sequentially processed by in situ hybridization for target gene expression and immunostained for retroviral infection.

(Row 1) Induction of *Spry1* expression in anterior limb mesenchyme. Overlay of bright field image (false colored green; original, left panel) and Fgfr1* virus show a large clone of *Spry1* + cells coincident with the infected cell clone (arrowheads).
(Rows 2,3) Induction of *Shh* expression in posterior limb mesenchyme. Overlay of bright field (false-colored green; original, left) and Fgfr1* virus show *Shh*+ cells coincident with the infected cell clones (arrowheads). Endogenous Shh domain is marked in Row 3 (arrow).

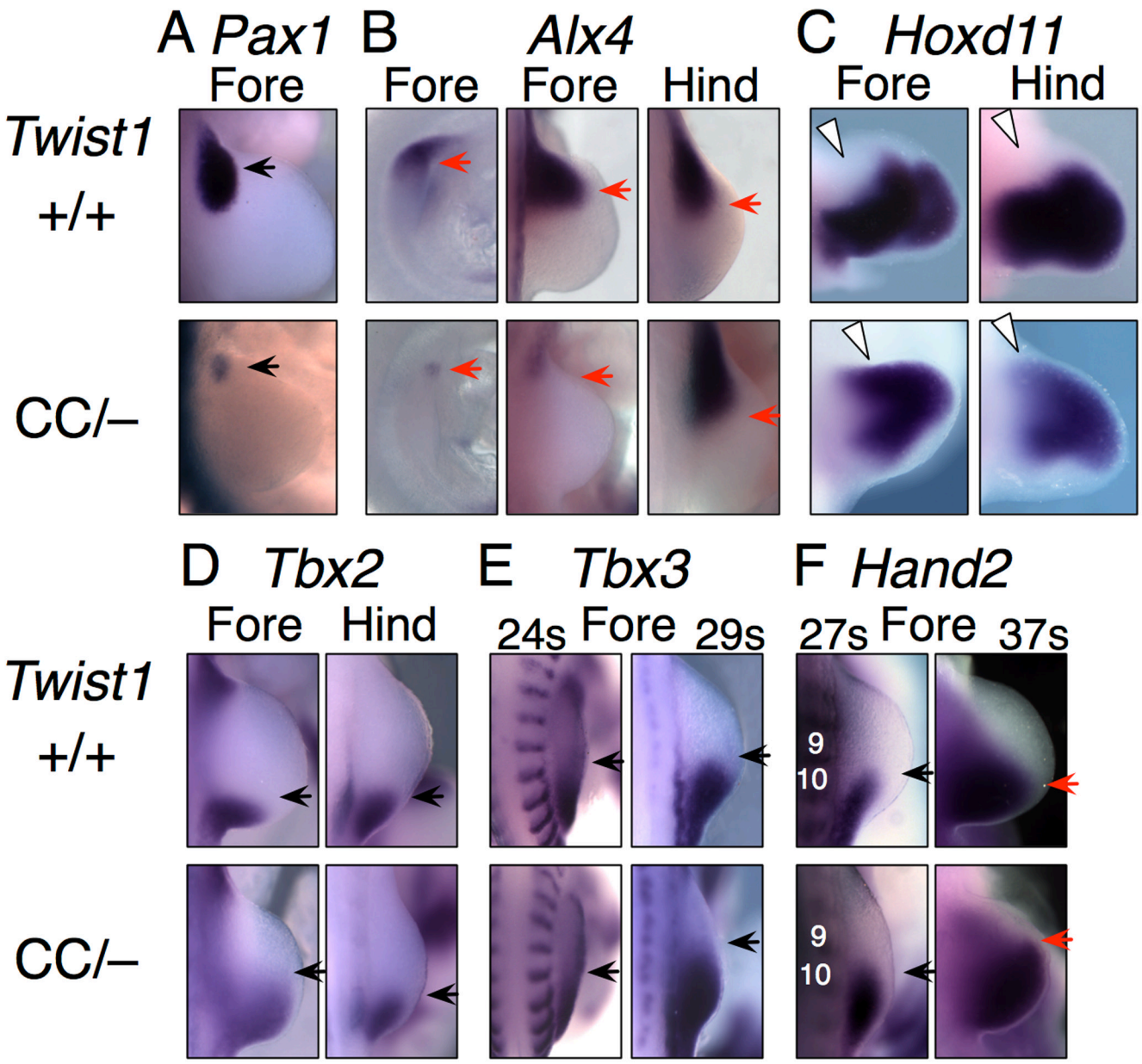

Figure 6. Regulation of transcription factor mRNA expression by *Twist1*

(A) Anterior-proximal *Pax1* is strongly downregulated (arrow) in mutant forelimb buds.

(B) *Alx4* is substantially downregulated at E9.25 (left column) and excluded from the forelimb mesenchyme by E10 (center), but is grossly unaffected in hindlimbs.

(C) *Hoxd11* is induced in anterior-proximal mutant limb buds at E11 (white arrowheads).

(D) Anterior boundary of *Tbx2* expression at e10 (black arrow) is shifted anteriorly in mutant forelimb, but not hindlimb.

(E) The anterior boundary of *Tbx3* is unchanged in *Twist1*$^{CC/-}$ forelimb at 24 somites, but is shifted anteriorly at 29 somites (E9.5–10).

(F) The anterior boundary of *Hand2* is unchanged in *Twist1*$^{CC/-}$ forelimb at 27 somites (black arrows), but is shifted anteriorly (red arrows) at 37 somites (E10.5). Somites 9 and 10 are indicated.

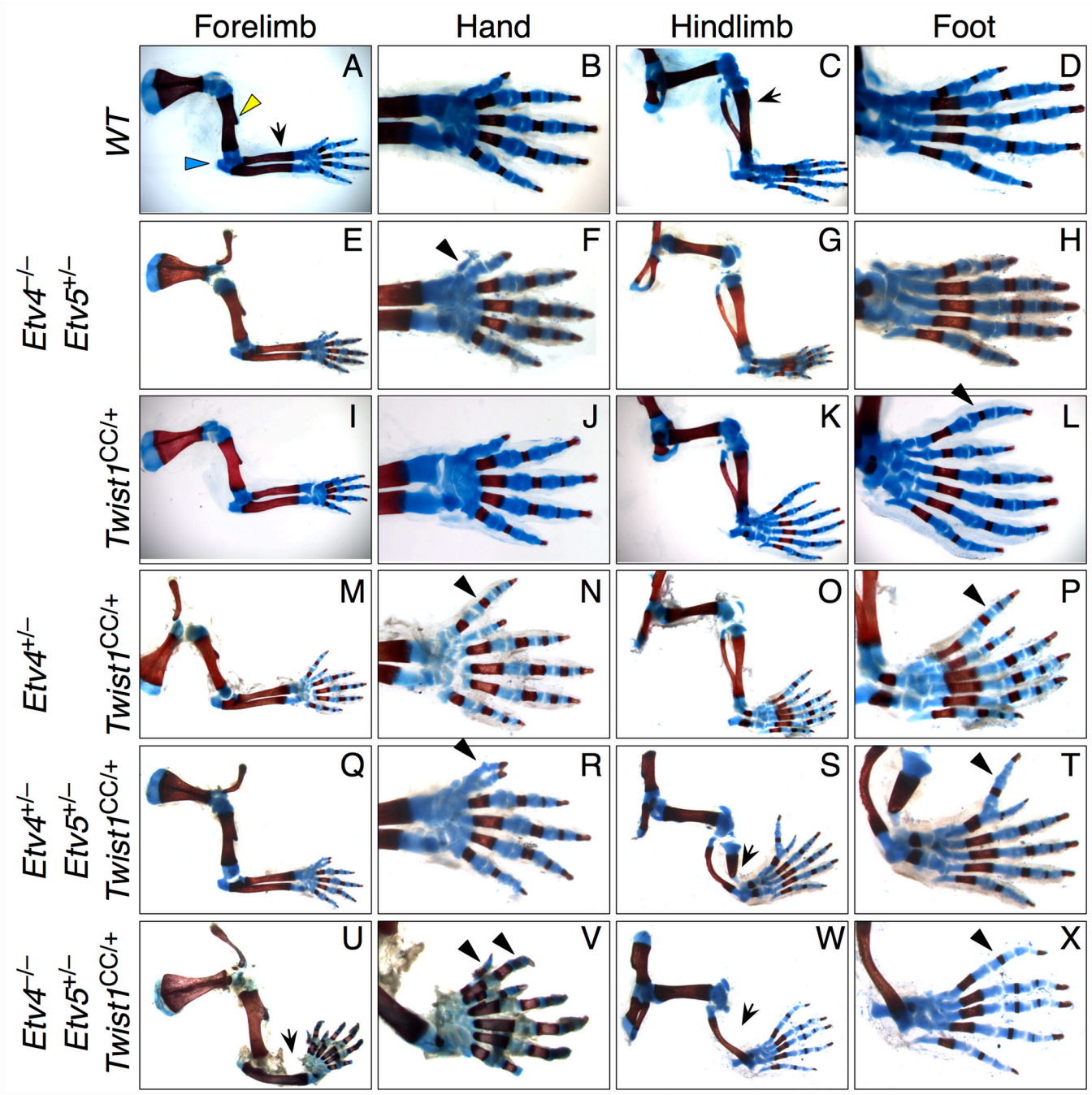

Figure 7. *Twist1* interacts genetically with Etv family genes

Limb skeletal patterns in progeny of *Twist1*$^{CC/+}$ intercrosses with *Etv4*$^{+/-}$ and *Etv5*$^{+/-}$ mice.
(A–D) Wild-type morphology, duplicated from Fig. 1.
(E–H) A small preaxial digit is occasionally present in *Etv4*$^{-/-}$*Etv5*$^{+/-}$ forelimbs (arrowhead).
(I–L) *Twist1*$^{CC/+}$ hindlimb preaxial polydactyly, duplicated from Fig. 1.
(M–P) Reducing *Etv4* or *Etv5* (see also Table 2) dosage in *Twist1*$^{CC/+}$ mutants causes posteriorized preaxial polydactyly of both forelimb and hindlimb (arrowheads).
(Q–R) *Twist1*$^{CC/+}$ mice lacking two *Etv4* or *Etv5* alleles have enhanced limb phenotypes, with preaxial polydactyly (arrowheads) and tibial hypoplasia (arrow).

(U–X) Removing three Etv gene copies phenocopies *Twist1*$^{CC/CC}$ limbs, with radial and tibial aplasia (arrows) and preaxial polydactyly (arrowheads). Note the humerus, including the deltoid tuberosity (yellow arrow, A), and proximal elements appear normal.

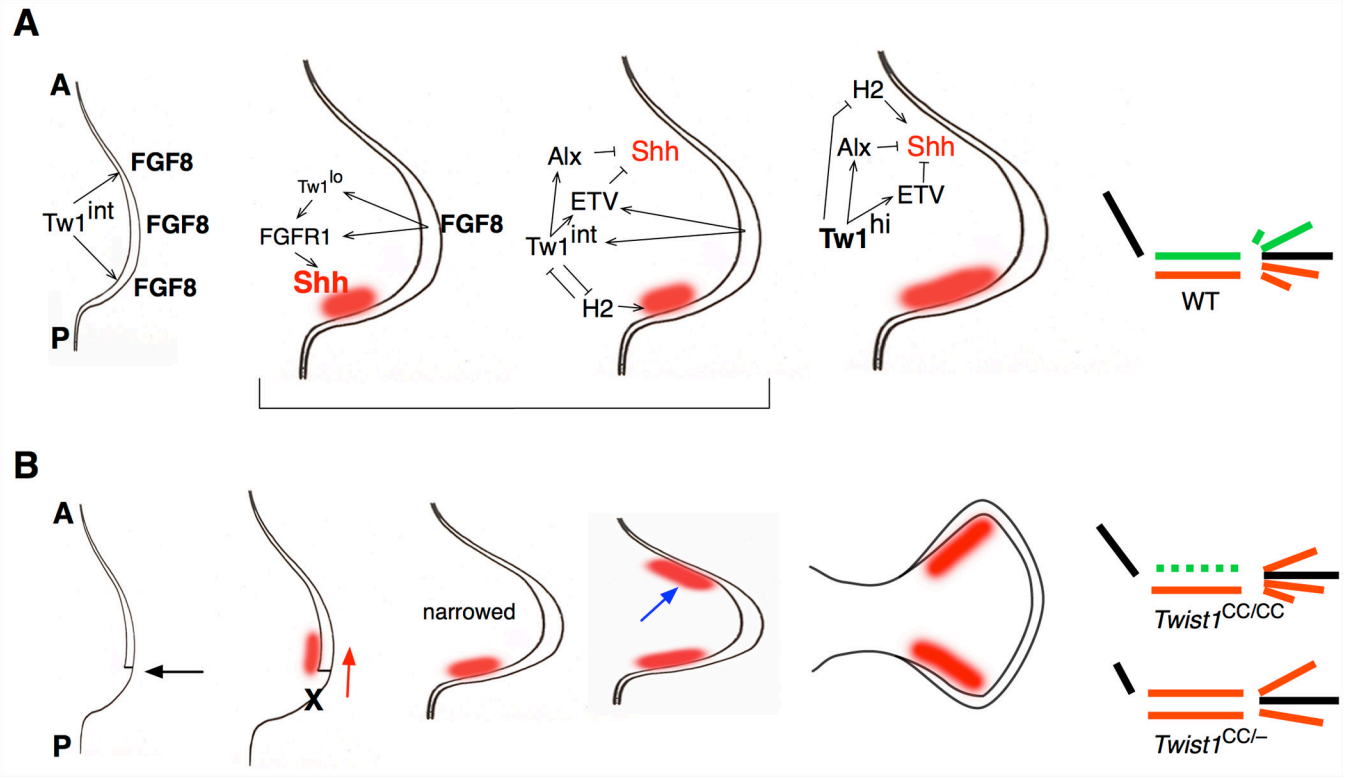

Figure 8. Model of *Twist1* function in early limb development

A. Summary of regulatory relationships between *Twist1* and downstream genes in the limb bud.

1st panel: Intermediate levels of Twist1 ($Tw1^{int}$) are required for *Fgf8* expression in the AER before *Shh* expression begins. 2nd and 3rd panels: FGF signals from the AER induce *Twist1* expression which itself maintains FGF receptor (FGFR1) expression. A minimal level of Twist1 activity ($Tw1^{lo}$) is required for FGF to induce robust *Shh* expression (red area). At the same time, intermediate Twist1 levels act through aristaless (Alx) and Etv family genes to suppress *Shh* expression in the anterior limb bud, while also maintaining *Shh* expression at the posterior of the bud by antagonizing Hand2 activity. 4th panel: High levels of Twist1 activity ($Tw1^{hi}$) suppress *Shh* expression in the anterior limb bud through the same gene network. Diagram: The result is a normally patterned limb, with an intact stylopod (black), two zeugopod bones, and five digits in the autopod. Anterior elements in green, posterior ones in red. A: anterior, P: posterior.

B. Developmental progression of $Twist1^{CC/CC}$ and $Twist1^{CC/-}$ limb phenotypes.

1st panel: When Twist1 activity is substantially reduced the AER is shortened, most importantly at the posterior (black arrow). 2nd panel: the reduced range and intensity of FGF signaling result in an anterior/distal shift in *Shh* expression (red arrow), while the posterior mesenchyme does not grow out (**X**). 3rd panel: Failed outgrowth of the limb margins leads to a narrower bud, with *Shh* at the new posterior margin. 4th panel: Derepressing *Shh* expression leads to an ectopic anterior *Shh* domain (blue arrow), with timing and magnitude proportional to reduction in Twist1 activity. 5th: This ectopic Shh extends the anterior AER, thus expanding the distal bud.

Diagram: In $Twist1^{CC/CC}$ mutants, the smaller bud supports only one zeugopod condensation, which is specified as posterior by Shh. In the forelimb autopod fewer elements condense, although this is partially rescued by anterior Shh, which posteriorizes these digits. In $Twist1^{CC/-}$ mutants, the initial reduction in the bud is more severe, but ectopic Shh initiates

earlier. This expands the presumptive zeugopod region allowing two condensations, along with posteriorization of the anterior element, resulting in a duplicated ulna. Anterior elements in the autopod are also posteriorized.

Dev Biol. Author manuscript; available in PMC 2011 November 1.

Table 1

Twist1 and Twist1/Hand2 mutant limb and girdle phenotypes

		HUMERUS/FEMUR[2]		RADIUS/TIBIA[2]			SCAPULA/PUBIS[2]	
	n[1]	Hypoplastic	Absent	Hypoplastic	Absent	Dup. Ulna/Fibula	Hypoplastic	Absent
Forelimb								
Twist1 +/+	10	–	–	–	–	–	–	–
Twist1 CC/+	20	–	–	–	–	–	–	–
Twist1 CC/CC	42	–	–	19%	81%	–	100%	–
Twist1 CC/−	12	100%	–	25%	8%	67%	100%	–
Twist1 CC/Fx, Prx-cre	6	100%	–	–	100%	–	100%	–
Twist1 Fx/Fx, Prx-cre	6	67%	33%	–	100%	100%	83%	17%
Twist1 CC/CC, Hand2 +/−	10	–	–	10%	90%	–	100%	–
Twist1 CC/−, Hand2 +/−	7	71%	–	14%	72%	14%	100%	–
Hindlimb								
Twist1 +/+	10	–	–	–	–	–	–	–
Twist1 CC/+	20	–	–	–	–	–	–	–
Twist1 CC/CC	37	–	–	–	100%	–	87%[4]	–
Twist1 CC/−	11	–	–	–	100%	–	100%[5]	–
Twist1 CC/Fx, Prx-cre	6	–	–	–	100%	–	33%	–
Twist1 Fx/Fx, Prx-cre	6	–	–	50%	33%	–	67%	–
Twist1 CC/CC, Hand2 +/−	8	–	–	–	100%	–	25%	–
Twist1 CC/−, Hand2 +/−	5	–	–	40%	60%	–	67%[6]	–

		NUMBER OF DIGITS[2]					
	n[1]	3	4	5	6	Presence of digit 1[2]	Normal A/P pattern[2,3]
Forelimb							
Twist1 +/+	10	–	–	100%	–	100%	100%
Twist1 CC/+	20	–	–	100%	–	100%	100%
Twist1 CC/CC	42	–	64%	36%	–	10%	–

	n[1]	NUMBER OF DIGITS[2] 3	4	5	6	Presence of digit 1[2]	Normal A/P pattern[2,3]
Twist1 CC/−	12	50%	25%	25%	–	9%	–
Twist1 CC/Fx, Prx-cre	6	17%	83%	–	–	–	–
Twist1 Fx/Fx, Prx-cre	6	–	67%	33%	–	–	–
Twist1 CC/CC, Hand2 +/−	10	–	50%	50%	–	–	–
Twist1 CC/−, Hand2 +/−	7	–	20%	70%	–	–	–
Hindlimb							
Twist1 +/+	10	–	–	100%	–	100%	100%
Twist1 CC/+	20	–	–	25%	75%	100%	25%
Twist1 CC/CC	37	–	–	100%	–	–	–
Twist1 CC/−	11	–	30%	70%	–	–	–
Twist1 CC/Fx, Prx-cre	6	–	–	100%	–	–	–
Twist1 Fx/Fx, Prx-cre	6	–	–	50%	50%	33%	17%
Twist1 CC/CC, Hand2 +/−	8	–	–	100%	–	–	–
Twist1 CC/−, Hand2 +/−	5	–	30%	70%	–	–	–

[1] values represent individual limbs

[2] – represents 0%

[3] Abnormal patterns include ectopic preaxial digits (CC/+ hindlimbs), loss of asymmetry (CC/CC or CC/− hindlimbs), or digit reductions and/or fusions combined with mirror symmetry across the A/P axis (CC/CC, CC/Fx, Fx/Fx or CC/− forelimbs).

[4] n=40 for pubis phenotypes

[5] n=12 for pubis phenotypes

[6] n=6 for pubis phenotypes

Table 2

Compound *Twist1*^{CC} and *Etv4*/*Etv5* mutant limb and girdle phenotypes

Genotype				HUMERUS/FEMUR[1]		RADIUS/TIBIA[1]			SCAPULA/PUBIS[1]	
***Twist1* (C)**	***Etv4* (4)**	***Etv5* (5)**	**Abbreviation**	**n limbs**	**Hypoplastic**	**Hypoplastic**	**Absent**	**Dup. Ulna/Fibula**	**Hypoplastic**	**Absent**
Forelimb										
+/+	+/+	+/+	Wild-type	8	–	—	–	–	–	–
+/+	+/–	+/+	4	8	–	—	–	–	–	–
+/+	+/+	+/–	5	8	–	—	–	–	–	–
+/+	–/–	+/+	44	8	–	—	–	–	–	–
+/+	–/–	+/–	445	4	–	—	–	–	–	–
CC/+	+/+	+/+	C	22	–	—	–	–	–	–
CC/+	+/–	+/+	C4	22	–	—	–	–	–	–
CC/+	+/+	+/–	C5	8	–	—	–	–	–	–
CC/+	–/–	+/+	C44	14	–	—	–	–	–	–
CC/+	+/–	+/–	C45	10	–	13%	–	–	–	–
CC/+	–/–	+/–	C445	4	–	25%	25%	–	–	–
Hindlimb										
+/+	+/+	+/+	Wild-type	8	–	—	–	–	–	–
+/+	+/–	+/+	4	8	–	—	–	–	–	–
+/+	+/+	+/–	5	8	–	—	–	–	–	–
+/+	–/–	+/+	44	8	–	—	–	–	–	–
+/+	–/–	+/–	445	4	–	—	–	–	–	–
CC/+	+/+	+/+	C	22	–	—	–	–	–	–
CC/+	+/–	+/+	C4	22	–	—	–	–	–	–
CC/+	+/+	+/–	C5	8	–	25%	–	–	–	–
CC/+	–/–	+/+	C44	14	–	29%	7%	–	–	–
CC/+	+/–	+/–	C45	10	–	50%	50%	–	–	–
CC/+	–/–	+/–	C445	4	–	–	100%	–	–	–

					NUMBER OF DIGITS[1]				Presence of digit 1	Normal A/P pattern[1]
					4	5	6	7		
Forelimb										
+/+	+/+	+/+	Wild-type	8	–	100%	–	–	100%	100%
+/+	+/−	+/+	4	8	–	100%	–	–	100%	100%
+/+	+/+	+/−	5	8	–	100%	–	–	100%	100%
+/+	−/−	+/+	44	8	–	100%	–	–	100%	100%
+/+	−/−	+/−	445	4	–	75%	25%	–	100%	75%
CC/+	+/+	+/+	C	22	–	100%	–	–	100%	100%
CC/+	+/−	+/+	C4	22	–	82%	18%	–	100%	82%
CC/+	+/+	+/−	C5	8	–	87%	13%	–	100%	87%
CC/+	−/−	+/+	C44	14	–	93%	7%	–	100%	93%
CC/+	+/−	+/−	C45	10	–	30%	70%	30%	100%	30%
CC/+	−/−	+/−	C445	4	–	–	50%	50%	100%	–
Hindlimb										
+/+	+/+	+/+	Wild-type	8	–	100%	–	–	100%	100%
+/+	+/−	+/+	4	8	–	100%	–	–	100%	100%
+/+	+/+	+/−	5	8	–	100%	–	–	100%	100%
+/+	−/−	+/+	44	8	–	100%	–	–	100%	100%
+/+	−/−	+/−	445	4	–	100%	–	–	100%	100%
CC/+	+/+	+/+	C	22	–	14%	86%	–	100%	14%
CC/+	+/−	+/+	C4	22	–	9%	86%	5%	100%	9%
CC/+	+/+	+/−	C5	8	–	–	100%	–	100%	–
CC/+	−/−	+/+	C44	14	–	7%	86%	7%	100%	7%
CC/+	+/−	+/−	C45	10	–	–	70%	30%	90%	–
CC/+	−/−	+/−	C445	4	–	–	100%	–	50%	–

[1] – represents 0%